

170573

BOĞAZIÇI UNIVERSITY
KANDİLLİ OBSERVATORY AND EARTHQUAKE RESEARCH INSTITUTE

**THE ANALYSIS OF 2003 SAROS EARTHQUAKE
SEQUENCE, NORTH EASTERN AEGEAN
REGION
&
A CALIBRATION STUDY OF SURFACE WAVE
MAGNITUDE (M_s)**

**MASTER OF SCIENCE THESIS BY
Ahu MUTLU**

Department: Geophysical Engineering

Programme: Geophysical Engineering

Advisor: Doç. Dr. Hayrullah KARABULUT

JANUARY 2005

BOĞAZİÇİ UNIVERSITY
KANDİLLİ OBSERVATORY AND EARTHQUAKE RESEARCH INSTITUTE

**THE ANALYSIS OF 2003 SAROS EARTHQUAKE
SEQUENCE, NORTH EASTERN AEGEAN REGION
&
A CALIBRATION STUDY OF SURFACE WAVE
MAGNITUDE (M_s)**

MASTER OF SCIENCE THESIS BY
Ahu MUTLU
2000700322

Date of defence examination : 5 January 2005

Supervisor :

Doç. Dr. Hayrullah KARABULUT

Members of the Examining Committee :

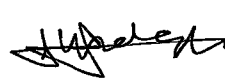
Doç. Dr.

Hayrullah KARABULUT



Doç. Dr.

Serdar ÖZALAYBEY



Prof.Dr.

Mustafa AKTAR



JANUARY 2005

TABLE OF CONTENTS

ACKNOWLEDGEMENTS	iii
ABSTRACT	iv
ÖZET	v
LIST OF FIGURES	vi
LIST OF TABLES	ix
LIST OF SYMBOLS	x
ABBREVIATIONS	xi
PART 1	
1.1. INTRODUCTION	1
1.2. DATA AND SEISMIC ACTIVITY	6
1.3. LOCATION OF EVENTS	12
1.4. FOCAL MECHANISMS	20
1.5. CONCLUSION	24
PART 2	
2.1. INTRODUCTION	25
2.1.1. SURFACE WAVE MAGNITUDE SCALE	29
2.2. DATA	33
2.3. ANALYSIS AND DISCUSSIONS	41
2.4. CONCLUSION	47
REFERENCES	48
APPENDIX A	51
APPENDIX B	58
APPENDIX C	67
APPENDIX D	69

ACKNOWLEDGEMENTS

I benefited greatly from the guidance and encouragements of Doç. Dr. Hayrullah KARABULUT. He suggested the subject and supplied many valuable insights. I would like to express my sincere appreciation to him.

I am indebted to Esen ARPAT and Prof. Dr. Mustafa AKTAR for discussions and many valuable comments.

I would like to thank the department of Geophysics for providing a good working environment.

With appreciation, I would like to thank Doç. Dr. Serdar ÖZALAYBEY for many valuable contributions and Cengiz TAPIRDAMAZ for his time to fulfill my hunger for data.

From the start of my work at Kandilli Observatory, Dean Childs had a major role of many aspects of my activities. I would like to thank him for his effort and patience.

I gratefully acknowledge Boğaziçi University, Kandilli Observatory and Earthquake Research Institute, Seismology Laboratory, TÜBİTAK, Marmara Research Center and National Observatory of Athens for providing waveform data.

This study benefited from a bilateral project between Turkey and Greece funded by TÜBİTAK from the Turkish side and the General Secretariat of Research and Technology (Ministry of Development) from the Greek side.

I would like to thank principal investigations of the project, Dr. Anastasia KIRATZI and Prof. Dr. Mustafa AKTAR.

Lastly, I would like to thank to my dear husband and my parents for their love and patience.

ABSTRACT

This study includes works on two different topics. In the first part, we analyzed the aftershock activity following $M_w=5.8$, 6th July 2003 Saros earthquake. The activity took place along the axis of the Saros gulf between the depths of 8 km and 20 km. The mainshock occurred at a depth of 17.5 km on the continuation of the North Anatolian Fault Zone (NAFZ) in the Gulf of Saros. Focal mechanism of the mainshock and largest aftershocks are almost pure right lateral strike slip with minor normal faulting. Strikes of the fault mechanism solutions are aligned with the axis of Saros depression.

In the second part of this study, three different surface wave magnitude (M_s) formulae, Prague, Herak and Herak and Modified Prague formulae were used to determine M_s for earthquakes in and around Turkey between the years 1997 and 2004, recorded at local and regional distances. The results of three M_s formulae with different correction factors were compared. It was concluded that Prague formula and Modified Prague formula produce significantly distance dependent estimates while Herak and Herak formula has no significant distance dependency and more robust M_s values. It was also observed that Herak and Herak formula has better correlation with Moment magnitude than the other two formulae.

ÖZET

Yüksek Lisans Tezi olarak yapılan bu çalışma birbirinden bağımsız iki bölümden oluşmaktadır. İlk bölümde 6 Haziran 2003 tarihinde Saros Körfezi'nde meydana gelen $M_w=5.8$ büyüklüğündeki depremin artçı sarsıntı dağılımının yerlerinin yeniden belirlenmesine çalışılmıştır. Deprem aktivitesi körfez doğrultusunda 8 km ile 20 km derinliktedir. Ana sarsıntı 17.5 km derinde ve Kuzey Anadolu Fay Hattı doğrultusunda meydana gelmiştir. Ana sarsıntının ve ardından meydana gelen en büyük artçı sarsıntıların mekanizma çözümü normal birleşeni olan baskın sağ yanal atımlı karakterlidir. Fay düzleminin bu karakteristiği Saros körfezindeki depresyon ve Kuzey Anadolu Fay Hattı uzanım doğrultusu ile uyumluluk gösterir.

İkinci bölümde, Prague, Herak ve Herak ve Modified Prague olarak adlandırılan üç farklı yüzey dalgası büyüklüğü (M_s) formülü, 1997 ve 2004 yılları arasında Türkiye ve çevresinde meydana gelen yerel ve bölgesel uzaklıktaki depremlerin M_s değerlerinin hesaplanması amacıyla kullanılmıştır. Farklı düzeltme değerlerindeki bu üç M_s formülü birbirleriyle karşılaştırılarak Prague formülü ve Modified Prague formülünün uzaklık bağımlılığı gösterirken, Herak ve Herak formülü zaman bağımlı değildir. Diğer yandan, Moment Magnitüdü (M_w) açısından yapılan değerlendirmelerde Herak ve Herak formülü diğer iki formüle göre daha iyi korelasyon gösterdiği görülmüştür.

LIST OF FIGURES

Figure 1.1	: Tectonic map of the eastern Mediterranean region (Kurt et al., 2000).....	1
Figure 1.2	: Topography and bathymetry features of the Northeast Europe Region. Faults are from Le Pichon et al. (2001).....	2
Figure 1.3	: Isoleismal map of the earthquake of 9 August 1912 prepared by Macovei (1912) in terms of the Rossi-Forel scale.....	3
Figure 1.4	: The seismic activity in the Northeast Aegean region between the years 1900 - 2003.....	5
Figure 1.5	: Regional map showing the location of the permanent stations operated by National Observatory of Athens, University of Thessaloniki, TUBITAK, Marmara Research Center and Boğaziçi University Kandilli Observatory and Earthquake Research Institute.....	7
Figure 1.6	: Map shows the location of the seismic stations operated by different Institutes (Figure 1.5) at epicentral distances less than 200 km.....	8
Figure 1.7	: Total number of earthquakes occurred between 5 June 2003 and 30 June 2003 and the earthquakes used in this study.....	9
Figure 1.8	: Vertical component of seismograms recorded at the station of Marmara Island (MRMX) for 6 selected earthquakes.....	10
Figure 1.9	: North-South component of seismograms recorded at the station of Marmara Island (MRMX) for 6 selected earthquakes.....	11

Figure 1.10	: East-West component of seismograms recorded at the station of Marmara Island (MRMX) for 6 selected earthquakes.....	11
Figure 1.11	: The velocity model developed for the Marmara region by Özalaybey et al. (2002).....	13
Figure 1.12	: Map (upper) and depth view (lower) along three profiles of the events between 5 July, 2003 and 15 June 2004 for 96 earthquakes by using velocity model for Marmara Sea.....	14
Figure 1.13	: Three initial velocity models (left) and three final velocity models (right).....	15
Figure 1.14	: Final velocity model used to relocate the events.....	16
Figure 1.15	: Map view and depth section of the located events following the Saros earthquake between 6 July, 2003 and 9 September 2003.....	17
Figure 1.16	: The maximum and minimum axes of the uncertainty ellipses of the aftershocks.....	18
Figure 1.17	: Depth errors for 96 of relocated earthquakes.....	19
Figure 1.18	: Focal mechanism of the mainshock.....	21
Figure 1.19	: Lower hemisphere projection of focal mechanisms of the mainshock and large aftershocks distribution (above). Green circles in the depth section show the selected events (below). Seismogenic zone circled with a rectangle.....	23
Figure 2.1	: Estimated decay of $\log(A/T)$ with distance compared to smoothed curve; theoretical curve (Thomas et al., 1977).....	27
Figure 2.2	: $\log(\Delta)$ +constant term of each formula versus epicentral distance were represented by different colors. Prague Formula, Herak and Herak Formula, Modified Prague Formula.....	32

Figure 2.3	: The selected earthquakes used in M_S calculations and listed in Table 2.1 which occurred between 1997 and 2004.....	35
Figure 2.4	: The station distribution used in M_S calculation.....	36
Figure 2.5	: Steps in M_S calculation.....	37
Figure 2.6	: Vertical component recording of the earthquake occurred in Greece at 14 August 2004 ($M_W=6.3$) which recorded at Isparta (ISP) station, Filtered with a bandpass filter of 18-22 sec., Filtered velocity seismogram converted to displacement, Filtered velocity and displacement seismogram in the marked area.....	39
Figure 2.7	: Vertical component recording of the earthquake occurred in Greece on 14 August 2004 ($M_W=6.3$) which recorded at Portugal (MTE) station, Filtered with a bandpass filter of 18-22 sec., Filtered velocity seismogram converted to displacement, Filtered velocity and displacement seismogram in the marked area.....	40
Figure 2.8	: M_S values of the Bingöl ($M_W=6.4$) earthquake as a function of epicentral distance.....	42
Figure 2.9	: Surface wave magnitudes deviation from average M_S values as a function of epicentral distance using the Prague Formula.....	43
Figure 2.10	: Surface wave magnitudes deviation from average M_S values as a function of epicentral distance using the Herak and Herak Formula.....	44
Figure 2.11	: Surface wave magnitudes deviation from average M_S values as a function of epicentral distance using the Modified Prague Formula.....	45
Figure 2.12	: M_W versus M_S for Prague Formula, Herak and Herak Formula, Modified Prague Formula.....	46

LIST OF TABLES

Table 1.1 : Selected earthquakes with focal mechanisms.....	22
Table 2.1 : Earthquakes analyzed in this study.....	33
Table 2.2 : List of earthquakes and M_s magnitudes for three formulae.....	41
Table A-1 : List of seismic stations, coordinates and station corrections used for Saros earthquake sequence analysis.....	51
Table A-2 : List of seismic stations with corrections used for Saros earthquake sequence analysis.....	54
Table A-3 : List of Earthquakes located in the Gulf of Saros.....	55
Table C-1 : List of stations used in M_s calculations.....	67

LIST OF SYMBOLS

$d(\Delta)$: Decay of surface wave
K	: Factor independent of distance
Δ^{-a}	: Loss of amplitude due to dispersion
$(\sin \Delta)^{-1/2}$: Geometrical spreading
$e^{(-k \Delta)}$: Loss of amplitude due to anelastic absorption
A	: Maximum amplitude
Δ	: Epicentral distance
S_c	: Station correction
$(A/T)_{\max}$: Maximum Amplitude/Period
\log	: Notation \log_{10}



ABBREVIATIONS

CZ	: Check Republic Seismic Network
GE	: GEOFON Network Code
HL	: NOA Network Code
IRIS	: The Incorporated Research Institutions for Seismology
IS	: Israel Seismic Network
ISP	: Isparta-Turkey Seismic Station Code
IU	: IRIS Network Code
KO	: Kandilli Observatory Network Code
KOERI	: Kandilli Observatory and Earthquake Research Institute
M_s	: Surface Wave Magnitude
M_w	: Moment Magnitude
M_L	: Local Magnitude
MRC	: TÜBİTAK, Marmara Research Center
MRMX	: Marmara Island Seismic Station Code
MTE	: Portugal Seismic Station Code
NAFZ	: North Anatolian Fault Zone
NE	: Northeast
NEIC	: National Earthquake Information Center
NL	: Netherlands Seismic Network
NOA	: National Observatory of Athens
ORFEUS	: Observatories and Research Facilities for European
PL	: Poland Seismic Network
SW	: Southwest
TK	: TÜBİTAK, Marmara Research Center Network Code Seismology

PART 1

The Analysis of 2003 Saros Earthquake Sequence, North Eastern Aegean Region



1.1. INTRODUCTION

The Northeastern Aegean Region has been studied by many scientists since it is one of the most seismically active and rapidly deforming areas on the continent. A major tectonic structure bisecting the region is the North Anatolian Fault Zone (NAFZ) which extends east-west for over 1600 km across Turkey (Figure 1.1). The zone starts from the Karliova, continues into the Marmara region, the Gulf of Saros and the Aegean Sea.

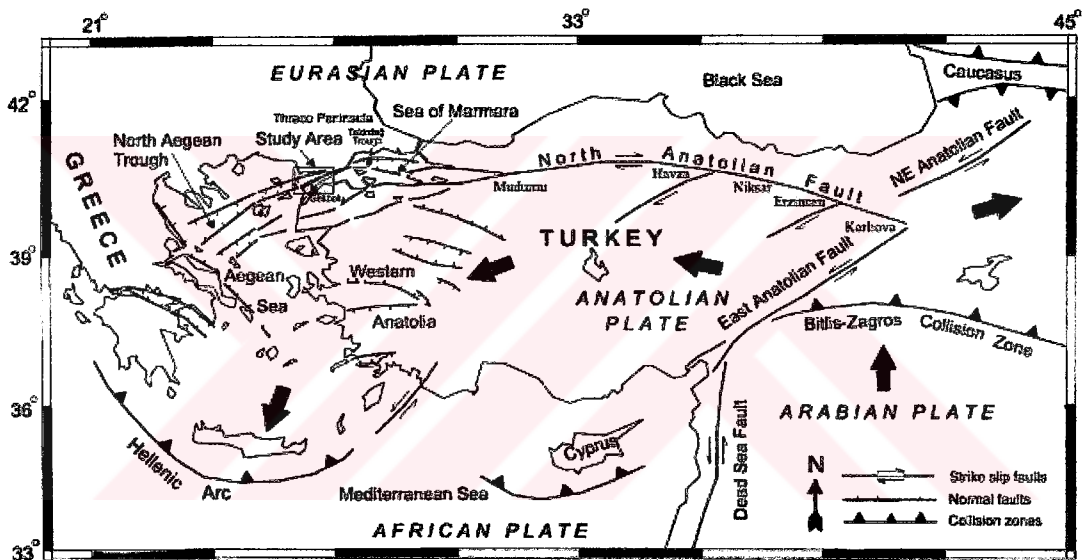


Figure 1.1: Tectonic map of the eastern Mediterranean region (Kurt et al., 2000).

The Gulf of Saros is an E-W trending neotectonic basinal structure located at the northeastern part of the Aegean Sea. The wedge-shaped Gulf extends parallel to the coasts of the Thrace shelf to the north and the Gelibolu peninsula to the south and widens and deepens toward WSW, where it becomes the easternmost part of the North Aegean Trough (Figure 1.2).

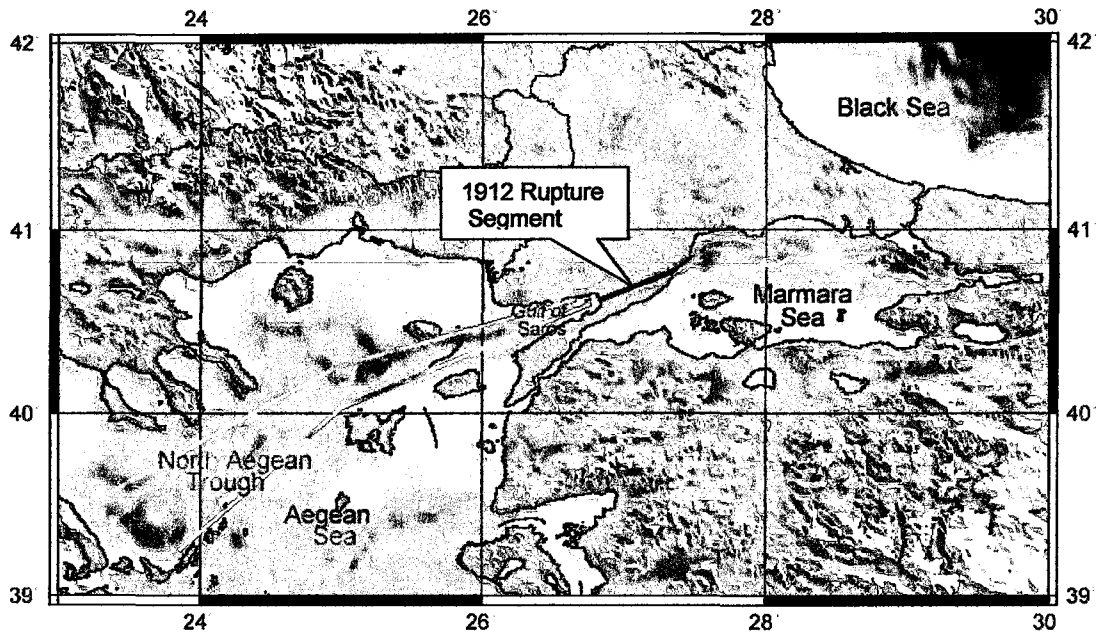


Figure 1.2: Topographic and bathymetric features of the Northeast Aegean Region. The red lines show the boundaries of North Aegean Trough. Faults in the Marmara Sea (pink lines) are from Le Pichon et al. (2001).

Many destructive earthquakes occurred in the region throughout history. Since the Gelibolu–Tekirdağ region is located along a trade route between Asia and Europe it has a well-recorded history going back to the 3rd century. 93, 484, 824, 1063 and 1343 AD are the years of some of the significant earthquakes (Ambraseys & Finkel 1986). The $M_w = 7.4$, 1912 Mürefte-Şarköy earthquake was one of the greatest earthquake in Europe during the 20th century. The largest event before 1912 occurred on 22 May 1766. The Mürefte-Şarköy earthquake on August 9, 1912 with magnitude 7.4 is one of the most significant seismic events in the Eastern Mediterranean, not only because of its large magnitude, but also because of its occurrence in one of the most densely populated parts of the Balkans. Despite its significance, however, there are few reports of this event (Ambraseys & Finkel 1986).

Izoseist maps were prepared from the macro seismic observations of 1912 Mürefte-Şarköy earthquake by different scientists. Macovei (1912), who did field study at the end of August 1912 pointed out that, stress area starts from Gaziköy village and passes through to the south shore of the Gulf of Saros through Gelibolu peninsula (Ambraseys & Finkel 1986). On the other hand, according to Mihailovic (1933), the biggest stress field is bounded with the eastern edge of the Gulf of Saros (Figure 1.3).

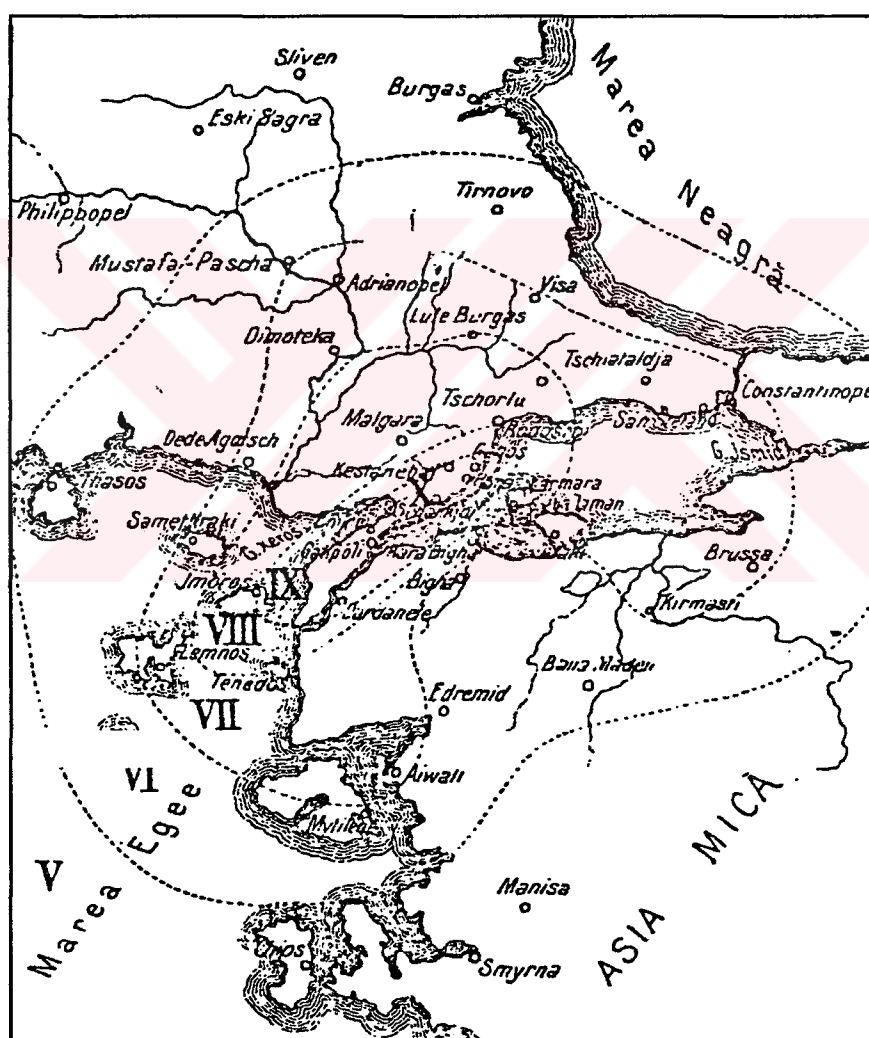


Figure 1.3: Isoseismal map of the earthquake of 9 August 1912 prepared by Macovei (1912) in terms of the Rossi-Forel scale.

Many studies have been done by different scientists on the geology, seismicity, tectonic regime of the Gulf of Saros. Çağatay et al. (1998) studied the region to reconstruct the geological evolution of the Gulf of Saros. They summarized the geological history of the gulf, on the basis of its tectonic settings, structural geology and stratigraphy. They concluded that, the Gulf of Saros is an Upper Miocene transtensional basin formed from the interaction between N-S extensional regime of the Aegean and NAF zone. Saatçılar et al. (1999) mapped the active faults in the north Aegean by using seismic reflection data in order to investigate present-day structure in the gulf. They reached to the conclusion that active fault zone at the north-central Aegean Sea region has dominantly normal fault mechanism and this region is in extensional regime. Another conclusion of the study was the active normal fault system cuts the Aegean Sea in a NE-SW direction, forming host and graben systems. Kurt et al. (2000) processed and interpreted 159 km multi-channel seismic reflection data in the gulf. They argued that, the dextral Ganos fault seems to play an essential role in forming the Gulf of Saros. Displacement along strike-slip faults produces a complex deformation zone. This deformation zone creates negative flower structure when the dip-slip component is normal and takes place normal to the main fault. The Ganos fault which caused 1912 earthquake is lying through the south of the Gulf of Saros with normal faults with dip-slip components and branches of that fault have negative flower structure. This negative flower structure occurred because of the tectonic escape of the NAF to the southwest and increased in relation to the subduction in the Hellenic arc.

No significant earthquake has occurred in the region since 1912, although a considerable number of earthquakes of small or medium magnitudes have occurred either in the Saros gulf or some distance out at sea. In 27 March 1975 an event with magnitude 6.7 took place in the Saros Gulf. On the westernmost end of this segment and approximately at the same location with 1975 earthquake, the most recent July 6,

2003 ($M_w=5.8$) Saros earthquake occurred. However no seismic activity was observed between the years 1900 and 2003 on the segment at which 1912 earthquake took place (Figure 1.4).

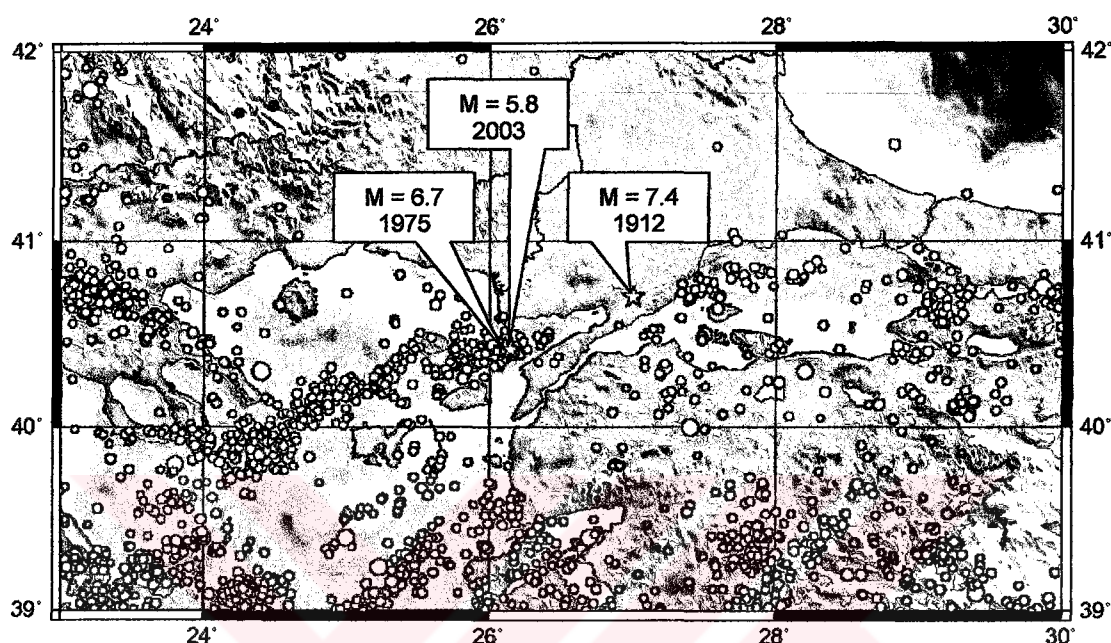


Figure 1.4: The seismic activity in the Northeast Aegean region between the years 1900 and 2003 (NEIC Catalog $M \geq 3.0$).

We studied the recent July 6, 2003 $M_w = 5.8$ earthquake in an effort to contribute to the understanding of the tectonic regime. This earthquake sequence has been recorded by many networks thus locations and focal mechanisms of the sequence are determined with good accuracy. Saros earthquake mainshock and its aftershocks (96 events) were relocated, local magnitudes were calculated and focal mechanisms of the large events ($M_L > 3.8$) were determined.

1.2. DATA AND SEISMIC ACTIVITY

A number of seismic networks have been operating in the Northern Aegean Region to monitor seismicity of the region. Kandilli Observatory and Earthquake Research Institute (KOERI) currently have 20 stations operating in the Marmara Region. TÜBİTAK, Marmara Research Center (MRC) operates a network in the Marmara Region with 30 stations. These two networks cover the eastern and southeastern azimuths of the study area. On the west and southwest of the study area the University of Thessaloniki (AUT) and the National Observatory of Athens (NOA) operate independent networks. In addition IRIS (The Incorporated Research Institutions for Seismology) and GEOFON stations are available all around the region. The station distributions are illustrated in Figure 1.5 and the type of the instruments are presented on Table A-1 in Appendix A.

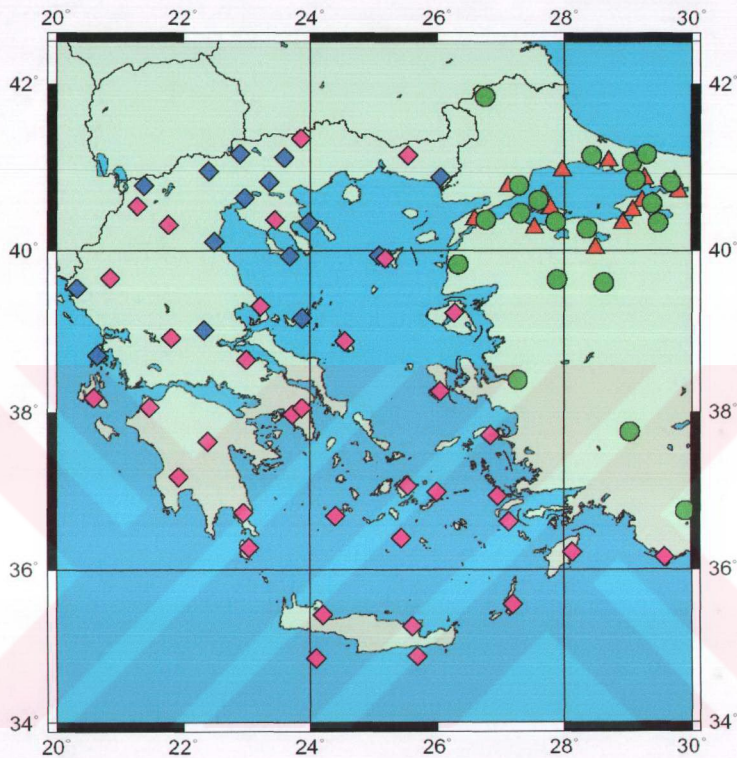


Figure 1.5: Regional map showing the location of the permanent stations operated by National Observatory of Athens (◆), University of Thessaloniki (◆), TÜBİTAK, Marmara Research Center (▲) and Boğaziçi University Kandilli Observatory and Earthquake Research Institute (●).

The mainshock occurred at the location of 40.427N, 26.103E, and 17.5 km. depth on July 6, 2003, 19:10:28:00 UTC. The aftershock sequence of this event was well recorded by more than 100 stations in and around the Aegean Sea and the western Turkey. The located events have good azimuthal station coverage with at least 4 stations at epicentral distance less than 100 km. Azimuthal gaps of the locations is varying between 65 and 259 degrees and average gap is 140 degrees. CEV (Cevizli) broadband seismic station is the closest station to the mainshock (40 km). Figure 1.6 shows the stations contributed to the locations at epicentral distances less than 200 km.

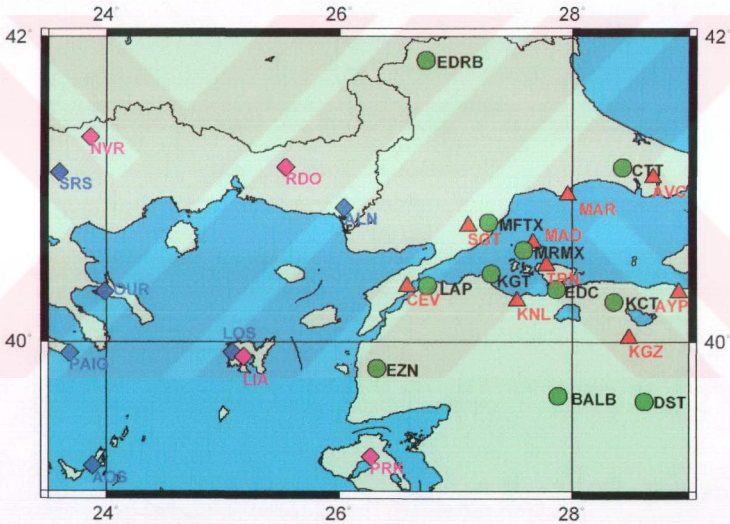


Figure 1.6: The location of the closest seismic stations to the epicentral area of the activity.

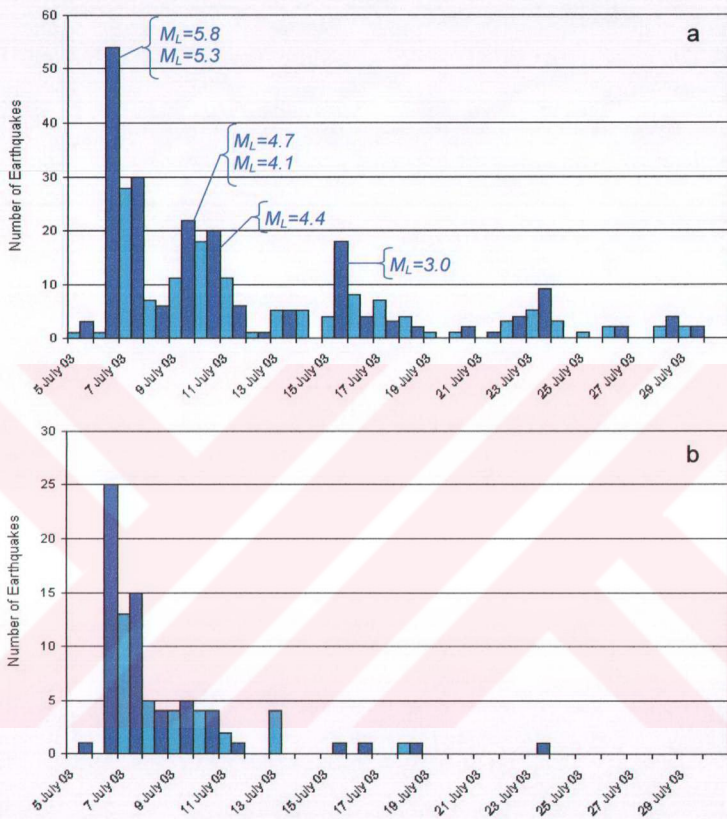


Figure 1.7: Total number of earthquakes occurred between 5 July 2003 and 30 July 2003 (a) and the earthquakes used in this study (b).

Figure 1.7 shows the total number of earthquakes and the number of earthquakes used in this study during the first month of the sequence. More than 12 aftershocks with magnitudes greater than 4 were detected during this period. The number of events is exponentially decaying in

time although we observe local increases following large aftershocks. A foreshock with a magnitude of 4.3 also occurred 21 hours before the mainshock.

Figures 1.8-1.10 shows three component seismograms of the foreshock, mainshock and some of the aftershocks recorded at Marmara Island seismic station (MRMX). The waveforms are aligned with P arrival times and normalized with the maximum trace amplitudes. The similarity among the waveforms for the first three traces and last three traces indicates clustering in two different areas.



Figure 1.8: Vertical component of seismograms recorded at the station of Marmara Island (MRMX) for 6 selected earthquakes.

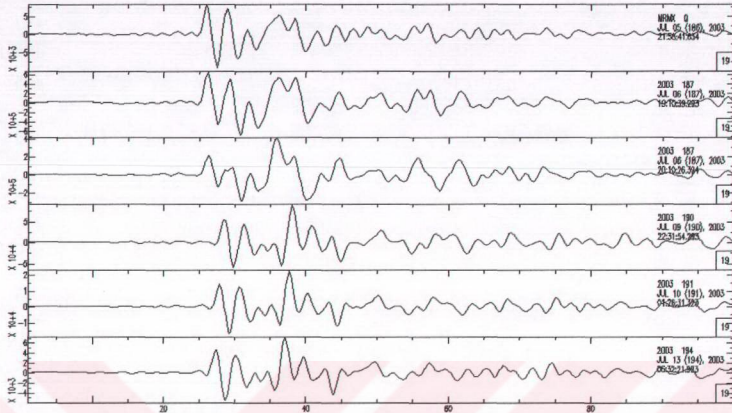


Figure 1.9: North-South component of seismograms recorded at the station of Marmara Island (MRMX) for 6 selected earthquakes.

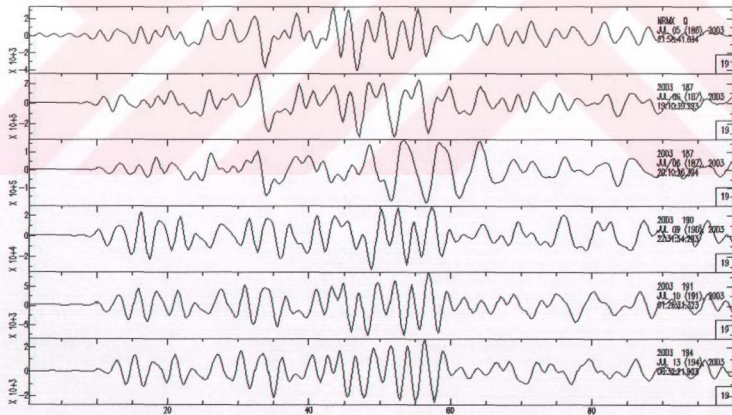


Figure 1.10: East-West component of seismograms recorded at the station of Marmara Island (MRMX) for 6 selected earthquakes.

1.3. LOCATION OF THE EVENTS

The waveforms from different networks were obtained and sorted into an event waveform database. The arrival times of P and S waves were picked manually by careful inspection of the vertical and horizontal seismograms. The similarity between waveforms was taken into account during the picking. This provided consistent picking among similar waveforms. Initially, 120 earthquakes were selected for the analysis. The selected earthquakes were recorded by at least 3 stations. The picking errors were less than 50 ms for large aftershocks but greater for smaller magnitude events. Earthquakes with large picking errors (> 90 ms) and large azimuthal gaps ($> 260^\circ$) were ignored and 96 earthquakes used for final analysis. In total, 1608 P phases and 909 S phases were used to locate 96 earthquakes. Local magnitudes were calculated from the broadband stations at distances less than 300 km. The magnitudes are calculated from the horizontal components and the maximum values at all stations were averaged. Local magnitudes of sequence are between 2.1 and 5.8. We also calculated M_S magnitude of mainshock and aftershocks with magnitude greater than 5.

Figure 1.11 shows the initial velocity model developed for the Marmara region (Özalaybey et al. (2002)). The model was used with the HYPO71 locating program (Lienert, 1994) and the average travel time RMS of 96 events was 0.26. The earthquakes located using the initial velocity model are illustrated in Figure 1.12.

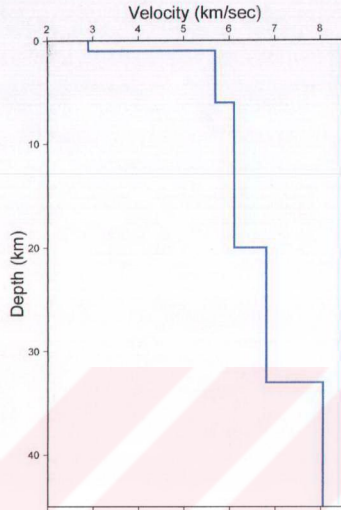


Figure 1.11: The initial velocity model used for locating events (Özalaybey et al. (2002)).

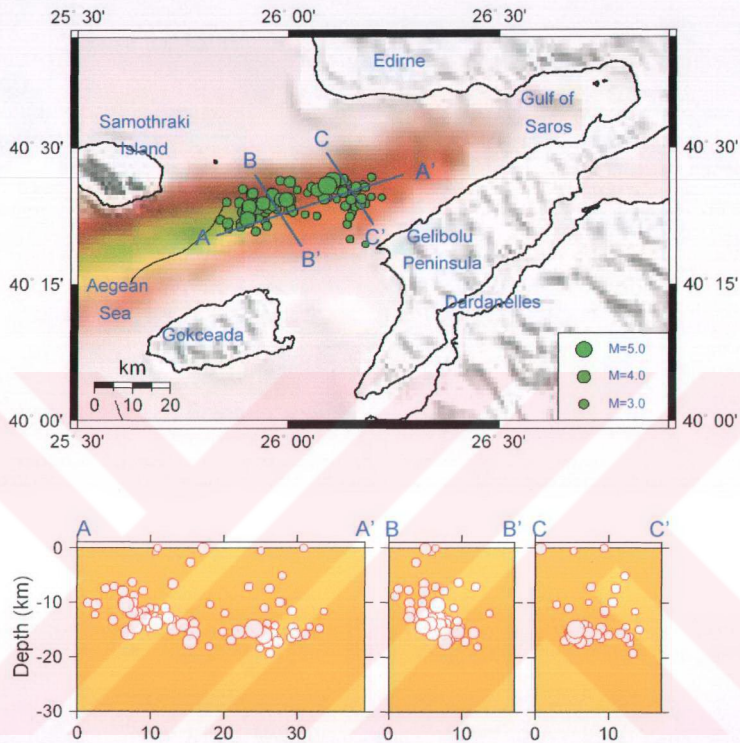


Figure 1.12: Map (upper) and depth view (lower) along three profiles of the events between 5 July, 2003 and 15 June 2004 for 96 earthquakes by using velocity model in Figure 1.11.

A new velocity model was obtained for the region using VELEST inversion code (Kissling et al. 1994) with a subset of the catalog. We selected 49 of 96 events recorded by more than 5 stations and RMS values less than 0.2. We created two more models from the perturbation of the model in Figure 1.11 to test the sensitivity of the inversion to initial models. V_p/V_s ratio was fixed to 1.73. Figure 1.13

illustrates three initial and three resulting velocity models. We also estimated station corrections from the inversion. The three initial velocity models converged to similar final models between the depth ranges of 10 and 30 km. This is expected since most of the aftershocks occurred below 10 km. There was a good correlation between station corrections and station sites. When a seismic station is located at hard rock site, station correction value is expected to be (-) residual. In contrast, station correction is expected to be (+) residual for the stations located at soft sites.

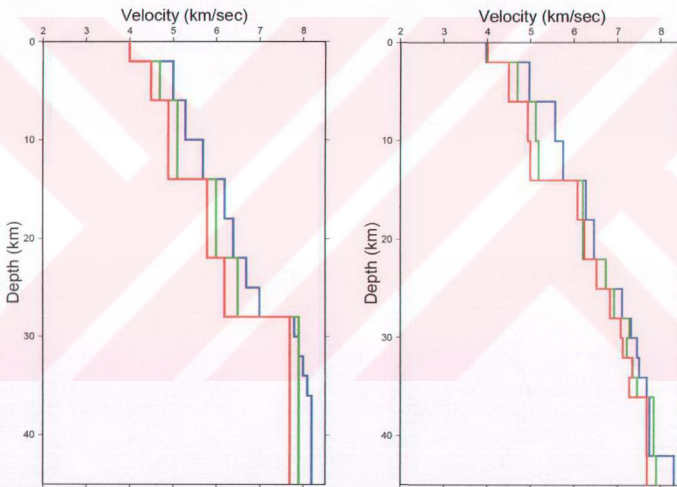


Figure 1.13: Three initial velocity models (left) and three final velocity models (right).

We relocated the events using the new velocity models and station corrections. The velocity model and station corrections providing minimum RMS residual (0.128) were used to relocate the events in the catalog of 96 events (Figure 1.14).

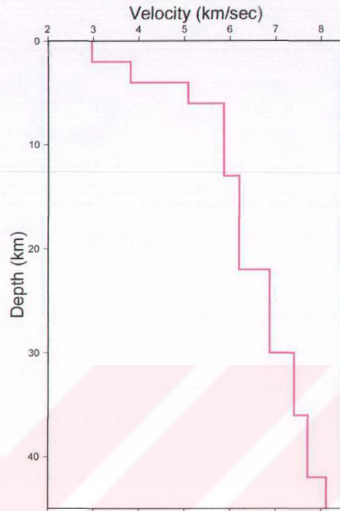


Figure 1.14: Final velocity model used to relocate the events.

Figure 1.15 shows the aftershock distribution obtained from the new velocity model. The distribution of the epicenters is aligned along the deep trough that forms the bathymetric axis of the Gulf. The aftershocks distribution defines approximately a 25 km long fault zone. Since the moment magnitude of the mainshock ($M_w=5.8$) is too small to create a 25 km fault zone the western part of the activity may be considered as triggered activity by the mainshock. No activity was detected on the northern side of the gulf and aftershocks clearly aligned on northern boundary of the trough. Relatively diffuse activity is observed in the south. Figure 1.15 depth section shows the depth distribution of the aftershocks. Three cross sections as A-A', B-B' and C-C' shows the aftershock distribution take place between the depths of 8 and 20 km.

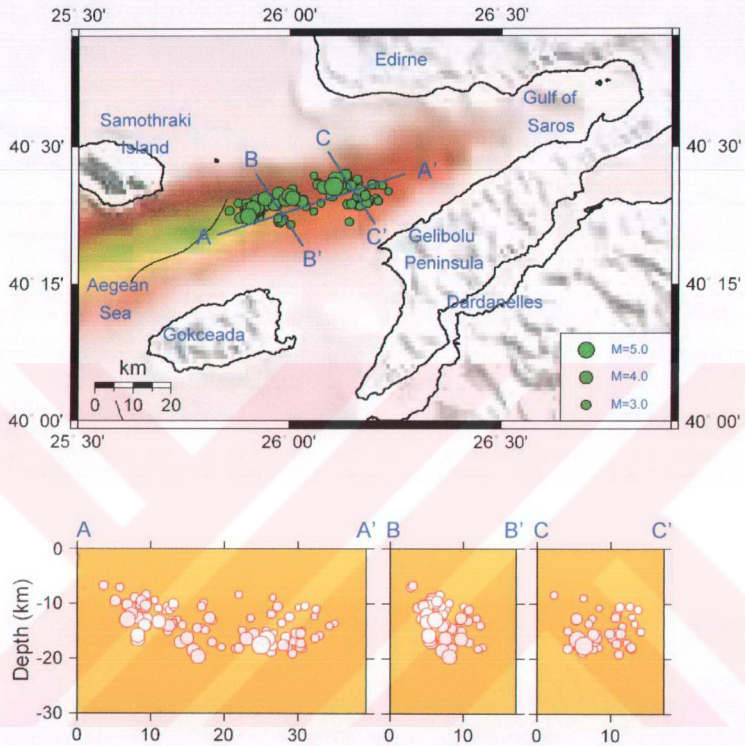


Figure 1.15: Map (upper) and depth view (lower) along three profiles of the events between 5 July, 2003 and 15 June 2004 for 96 earthquakes.

We calculated the uncertainties on the locations of the events. The major and minor axes of the ellipses are plotted in Figure 1.16. The results indicate that the errors are larger in N-S direction. This is not surprising since the number of stations located in the north and south is not as many as the number of the stations in the east and west. The average horizontal error is less than 2.5 km.

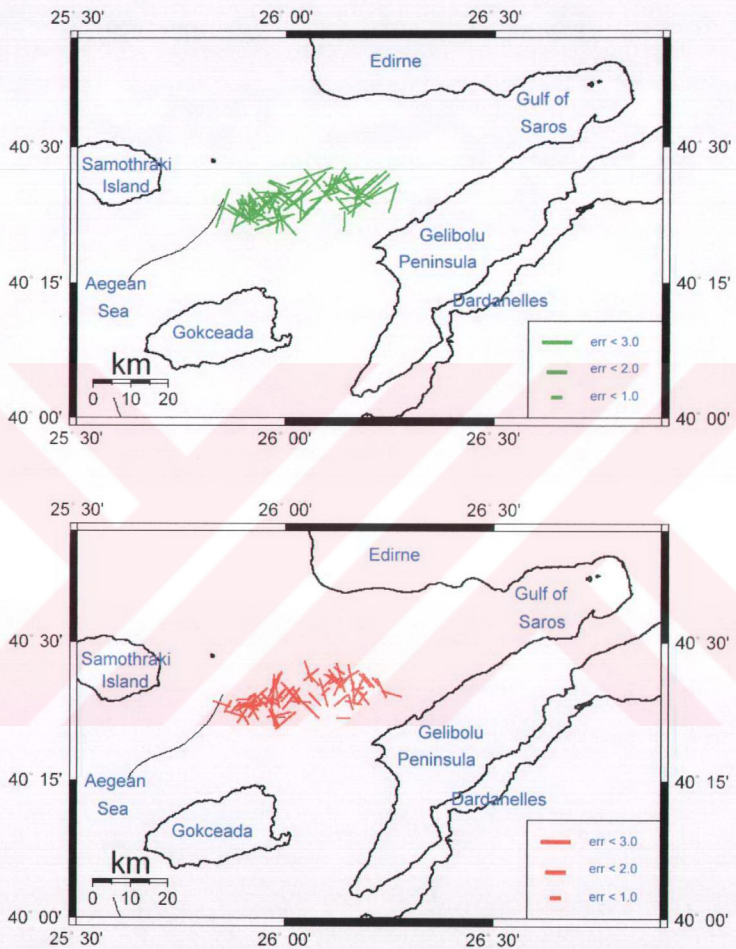


Figure 1.16: The maximum (above) and minimum (below) axes of the uncertainty ellipses of the earthquakes.

In the Figure 1.17 we plotted depth errors of each earthquake. Average vertical error is less than 3.5 km.

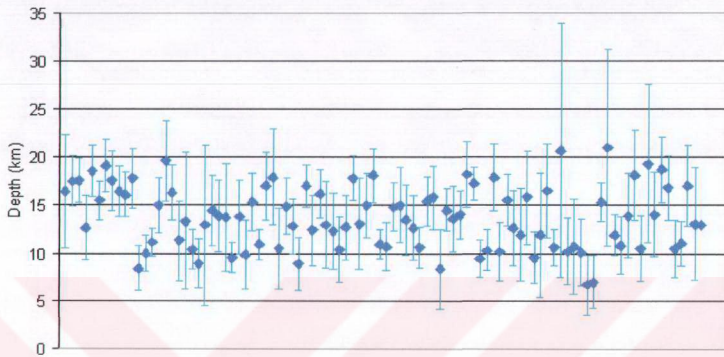


Figure 1.17: Depth errors for 96 of relocated earthquakes.

1.4. FOCAL MECHANISMS

Focal mechanisms of the well recorded events were obtained to reveal the style of faulting. Single-event, lower hemisphere focal mechanisms were determined using the FPFIT grid-search algorithm developed by Reasanberg and Oppenheimer (1985). Fifteen events with magnitudes greater than 3.8 were selected for focal mechanism determinations. The first motion polarities for each event were determined at more than fifteen stations. In total, 374 polarities were used while plotting the lower hemisphere for 15 selected events. Zero polarity errors were allowed with maximum 2 degrees grid search space.

Figure 1.18 shows the polarities and the focal mechanism of mainshock ($M_w=5.8$). 48 polarities were used in the solution. The source parameters for the mainshock strike= 345.5° , dip= 75.5° and rake= 4.0° . The estimated errors for the source parameters are small since the station coverage is good.

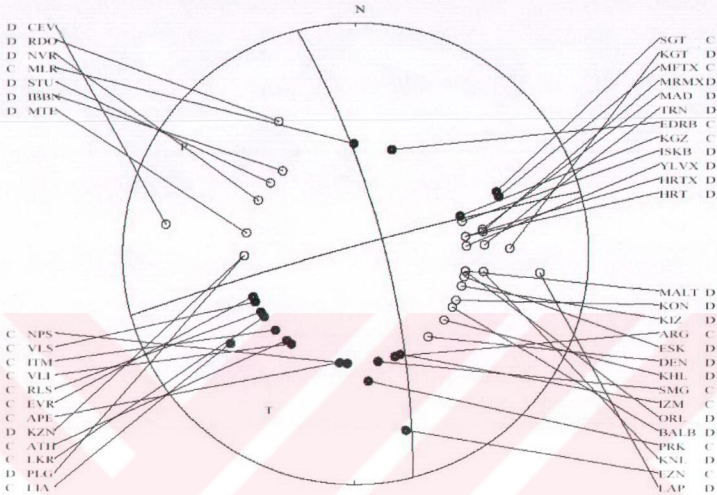


Figure 1.18: Focal mechanism of the mainshock. Filled circles show the compression and open circles shows dilatation.

The obtained focal mechanisms of the selected fifteen events are listed in Table 1.1 and shown in Figure 1.19. As shown in Figure 1.19, the focal mechanisms of selected earthquakes have dominant right lateral strike slip character with minor normal faulting components. The strike directions are in line with the bathymetric axis of the Gulf of Saros. The normal components show dipping to the south. This is consistent with the aftershock distribution which shows a diffused seismic activity to the south. The depth distribution below (Figure 1.19) shows the thickness of seismogenic zone which is around 12 km. The aftershock sequence direction is around N72S.

Table 1.1: Selected earthquakes with focal mechanisms.

Event Origin Time (yr.mn.dd hr:mn:sc.ms)	Latitude (N°)	Longitude (E°)	Depth (km)	M _L	Strike ± Stdev (°)	Dip ± Stdev (°)	Rake ± Stdev (°)
2003.07.05 21:58:29.60	40.441	26.063	11.7	4.3	80.0±1,8	90.0±0,1	150.0±1,6
2003.07.06 19:10:28.00	40.427	26.103	17.5	5.8	74.5±1,2	86.2±1,9	165.5±1,6
2003.07.06 20:10:15.60	40.439	26.108	16.4	5.3	80.6±1,2	70.3±1,3	-176.4±1,7
2003.07.06 20:48:53.30	40.406	26.006	19.6	4.7	63.7±3,5	64.3±5,4	-163.9±4,7
2003.07.06 22:05:48.50	40.403	25.989	16.3	4.2	86.7±4,8	79.5±4,0	145.4±3,8
2003.07.06 22:42:08.70	40.405	25.940	13.3	4.4	70.4±3,3	85.0±1,9	-171.3±3,2
2003.07.09 22:01:57.50	40.385	25.913	12.6	3.8	70.0±1,3	50.0±1,5	-180.0±2,2
2003.07.09 22:08:49.50	40.386	25.902	11.9	4.1	74.3±1,4	83.7±1,3	166.7±2,3
2003.07.09 22:31:40.70	40.388	25.912	15.8	4.7	99.5±2,4	44.0±1,6	-157.8±1,9
2003.07.10 01:26:17.70	40.387	25.912	16.5	4.4	80.3±1,0	81.1±4,5	-151.2±2,6
2003.07.10 09:01:17.80	40.183	25.305	20.7	4.0	76.1±9,2	72.9±7,9	-141.0±8,3
2003.07.13 06:32:08.10	40.389	25.923	13.9	4.0	68.5±0,2	60.5±0,7	174.3±0,1
2003.07.18 05:44:07.20	40.394	25.962	14.0	3.8	81.4±6,2	79.4±2,1	142.2±4,9
2003.08.31 07:50:56.70	40.415	25.972	17.0	4.0	77.8±4,2	44.0±3,0	-119.5±2,0
2004.06.15 12:02:38.50	40.373	25.901	12.9	5.1	74.1±4,5	67.5±4,7	-159.6±1,3

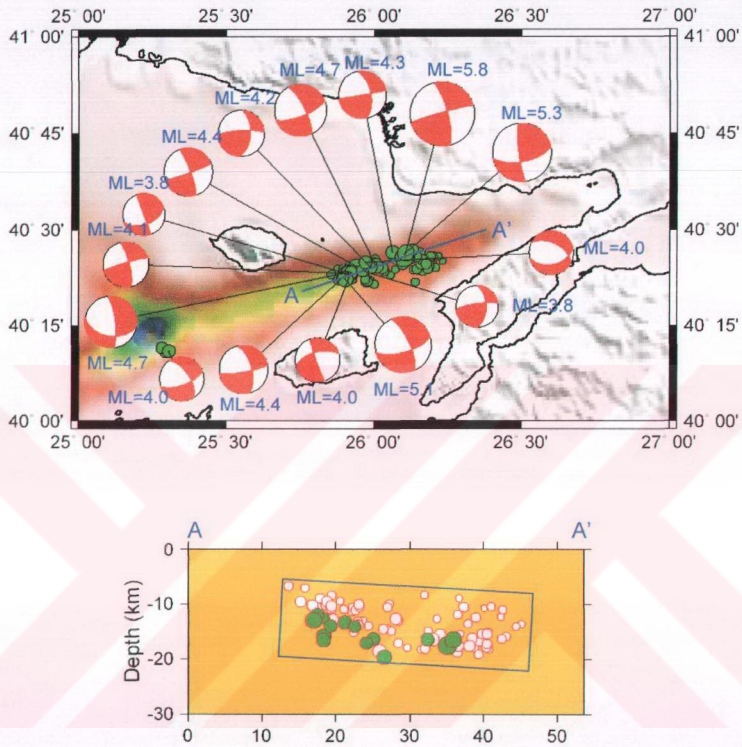


Figure 1.19: Lower hemisphere projection of focal mechanisms of the mainshock and large aftershocks distribution (above). Green circles in the depth section show the selected events (below). Seismogenic zone circled with a rectangle.

1.7. CONCLUSION

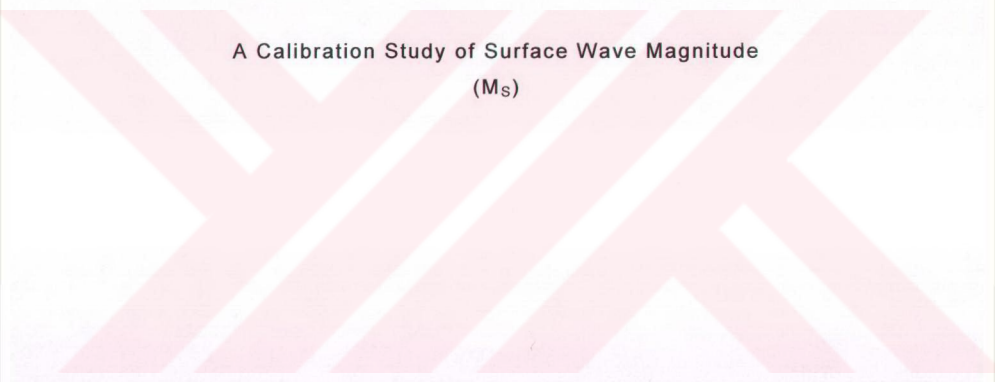
The 6th July 2003 Saros earthquake sequence occurred along the deep trough that forms the axis of the Gulf of Saros with 25 km long zone of aftershock activity. Thickness of the seismogenic zone is approximately 12 km. No seismic activity is detected on the northern shelf which may be the evidence for a stable non-deforming zone on the north of the Saros Bay. Contrasting with this, a relatively diffuse seismicity exists on the southern part of the depression. The main characteristic feature of the sequence is the right-lateral strike slip with minor normal component and aligned with the axis of the Saros depression, therefore with the North Anatolian Fault.

A relatively deep seismogenic zone which reaches 20 km clearly indicates that the activity is occurring well below the branching point of the flower structure (Kurt et al., 2000). This observation is not totally unexpected since a similar characteristic was also observed at the western end of the Marmara Sea (Özalaybey et al., 2002).

Another consideration is related to the argument of whether this well located swarm activity may represent the western limit of the 1912 rupture. It is well recognized that a consistent seismic quiescence line has established along the rupture length of the 1912 Ganos Earthquake ($M=7.4$). Although the total length of the aseismic line across the Ganos Fault agrees with the size of the 1912 event with the assumed constant slip, the exact location of the rupture endings will always be debatable. The swarm data presented in this study, unlike the earlier data, have the locations uncertainties of the order of 3 km horizontally; therefore indicate a well defined western limit to the quiescence line.

PART 2

**A Calibration Study of Surface Wave Magnitude
(M_s)**



2.1. INTRODUCTION

A quantitative measure of earthquake size was first invented by Charles Richter in the 1930's. After the installation of a network of high-quality seismographs in the Southern California, Richter realized that seismic wave amplitudes vary over a tremendous range and depends on epicentral distance. He studied the amplitude decay of seismic waves to correct the amplitudes for distance from epicenters. As a result, Richter proposed the "local magnitude scale", M_L , which today is still used to calculate magnitudes of California earthquakes. Richter and Gutenberg quickly realized that this concept should be applied to earthquakes worldwide. Gutenberg (1945) gave a formula based on maximum horizontal ground amplitudes, and from 1949 to 1959 various authors calculated similar empirical magnitude formula for different stations (cf. Bath, 1966). By the 1940's, M_S for all the larger earthquakes in the first half of the 20th century had been calculated by Gutenberg and Richter.

Hundreds of studies had been done by different seismologist after the years that Richter and Gutenberg gave a start for the idea of surface wave magnitude observations. As a result of these observations surface waves have been considered as a robust way to compute magnitudes. Observations showed that the most prominent signals recorded by a long-period seismograph for a distant shallow earthquake are surface waves with a period around 20 seconds. Because of stronger geometrical spreading, body waves show smaller amplitudes than surface waves. The surface waves with periods less than about 10 or 15 sec. suffer from scattering due to shallow heterogeneities and those with periods longer than 25 seconds begin to lose energy into the asthenosphere (Aki and Richards, 1980).

As realized by many scientists surface wave amplitude is decreases with the increase in distance. This decay has the form of

$h \log \Delta + \text{constant}$ which calls 'calibration function'. In this function h is a constant, Δ is epicentral distance. Soloviev (1955) proposed the use of the maximum ground particle velocity $(A/T)_{\max}$ instead of the maximum ground displacement A_{\max} and the corresponding calibration functions were obtained by Soloviev and Shebalin (1957), Vanek and Stelzner (1959), Christoskov (1965) and others.

Gutenberg (1945) and Vanek et al. (1962) showed that the calibration function to correct the decay of surface waves with distance approximates to a straight line with slope 1.66 when plotted against $\log \Delta$ at distances greater than 20° . However, the calibration function at short range appears to have a slope of 0.8 – 1.0 when plotted against $\log \Delta$, have been pointed out by von Seggern (1970); Evernden (1971) and Basham (1971), additionally Marshall & Basham (1972) published a composite curve combining a line with a slope of 0.8 at short range with a line of slope 1.66 at long range and joining these two lines of different slopes by a smooth curve. The work of Gutenberg (1945) and Vanek et al. (1962) is based on measurements horizontal components of ground motion. Since the Rayleigh wave particle motion has larger amplitudes in vertical components, it is preferred to calculate M_s from the vertical component of ground motion. Thomas et al. (1977) estimated a calibration function for M_s directly from the observed decay of the vertical component of surface waves over the distance range 0-150°. They showed the estimated decay of $\log (A_{\max}/T)$ for Rayleigh waves as a function of distance (Figure 2.1).

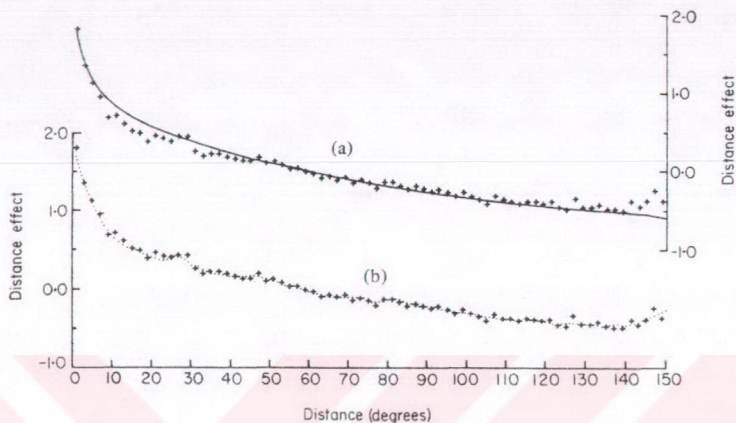


Figure 2.1: Estimated decay of $\log(A/T)$ with distance compared to (a) smoothed curve; (b) theoretical curve. + Estimated curve smoothed curve; — theoretical curve (Thomas et al., 1977).

To correct the decay in M_S calculations, they assumed that this decay has the form of $h \log \Delta + \text{constant}$ (h is a coefficient). Figure 2.1(b) shows an attempt to fit a theoretical curve of surface wave decay with distance. The decay $d(\Delta)$, of surface wave of a given period with epicentral distance Δ can be written as

$$d(\Delta) = K \Delta^{-a} (\sin \Delta)^{-1/2} e^{(-k \Delta)} \quad (2.1)$$

where K is some factor independent of distance, Δ^{-a} describes the loss of amplitude due to dispersion, $(\sin \Delta)^{-1/2}$ is the term for geometrical spreading and $e^{(-k \Delta)}$ describes the loss of amplitude due to anelastic absorption.

If the decay of $\log(A/T)$ is corrected for geometrical spreading and dispersion, the resulting curve should show a linear decay with Δ .

Therefore, they showed that the estimated decay is corrected for geometrical spreading and dispersion by assuming $a=1/2$. One of the conclusions that Thomas et al. (1977) drawn was the estimated calibration function has a slope as a function of $\log\Delta$ of roughly 0.8 at short ranges and 1.5 at long ranges. If the calibration function is assumed to have the form of $h\log\Delta+\text{constant}$, h is estimated to be 1.15. According to Okal (1989), the seismic moment is related to the time domain amplitude through the product of amplitude and period, rather than through their ratio, commonly used in many magnitude scales, including in the Prague formula (informed detailed in topic 2.1.1). The use of (A/T) stems from early attempts (e.g., Gutenberg and Richter, 1942) to measure the total elastic energy released by the earthquake source, the energy of a perfect harmonic oscillator being is proportional to A^2/T^2 . That magnitude measurements using (A/T) can occasionally be taken at periods other than the reference period reflects a partial compensation for a large number of period-dependent terms ignored in the Prague formula. The use of (A/T) cannot be justified theoretically for a strong dispersed wave. Furthermore, outside the narrow interval 17-23 sec., it is expected to lead to significant bias.

The effect for the dispersion of the wave and the effect for anelastic attenuation (also distance dependence) are period-dependent (Okal E., 1989). Dispersion affects amplitudes of the wave and controls the spreading with group time of energy in the frequency band. Both of these parameters are ignored in the Prague formula.

According to Herak and Herak (1993), the average difference between M_s values at small epicentral distances and those at large distances exceed 0.5 magnitude units. By the study of 5514 M_s readings they proposed that the relation is very close to the results of von Seggern (1977) and they concluded that the new calibration function for 20 sec. Rayleigh wave amplitude decreases as 1.094 times distance.

Rezapour and Pearce (1998) investigated bias in surface wave magnitude due to inadequate distance corrections by using the complete ISC (International Seismological Center) and NEIC (National Earthquake Information Center) data sets from 1978 to 1993. By comparing different M_S formulae, they reported that regional variations in instrumentation are distorting the perceived regional differences in M_S station residuals. They pointed the importance of applying a suitable distance correction term for M_S calculation.

Purpose of this study is to determine surface wave magnitudes for earthquakes occurring in and around Turkey from regional stations. In order to reach this goal we used three different M_S formulae called Prague, Herak and Herak and Modified Prague formula. Two alternative formulae have been tested against modified Prague formula and correlation with the M_W is searched. By using a proper correction at distances less than 20° , M_S values are calculated and compared to the results at distances greater than 20° .

2.1.1. SURFACE WAVE MAGNITUDE SCALES

Surface wave magnitude was originally defined by Gutenberg (1945) as the first attempt to measure the strength of shallow earthquakes at teleseismic distances. It was an extension of the local magnitude scale, M_L , introduced by Richter (1935) for the rating of regional earthquakes in California. The M_S scale was adjusted to agree with M_L and is based on 20 seconds surface waves from shallow earthquakes in the distance range of 15° and 130° . The final formula of Gutenberg (1945) is

$$M_S^{\text{Gutenberg}} = \log A + 1,656 \cdot \log (\Delta) + 1,818 + S_C \quad (2.2)$$

where S_C is a station correction, Δ is the epicentral distance in degrees and A is the maximum amplitude on the horizontal component

seismogram in microns for a surface wave with period of about 20 sec. This formula was originally designed to use amplitude data from horizontal seismographs.

Vanek et al. (1962) developed the "Prague Formula";

$$M_S^{\text{Prague}} = \log (A/T)_{\max} + 1,66 \cdot \log (\Delta) + 3,3 \quad (2.3)$$

where A is the vertical or resultant amplitude in microns and T is the mean period in seconds. $(A/T)_{\max}$ is the maximum of all A/T (Amplitude/Period) values of wave groups on a record. The Prague formula employed a geographic average of various distance normalizing terms and incorporated T in the formula to account for those cases. In this study, we chose the period constant as 20 sec. As a result, there is no significant difference between the values of $\log(A/T)_{\max}$ and $\log(A_{\max}/T)$.

Okal (1989) considered the theoretical issues of magnitude corrections in detail. He compared a theoretical distance correction with that of Prague formula and found that the difference between these corrections never exceeds ± 0.05 magnitude units for $20^\circ < \Delta < 150^\circ$. Okal found that, compared with the theoretical distance correction, the Prague distance correction overestimates M_S by between 0.02 and 0.04 magnitude units in the distance range 20° to 110° . Nevertheless, he concluded that the distance correction of the Prague formula was adequate except at very short distances.

None of the above formulae incorporate corrections that are theoretically predicted, despite the fact that the main contributions to both distance and depth corrections are known from seismological theory, as pointed out by Nuttli (1973). Theoretically the distance correction term is not logarithmic, therefore there is a limit to the distance range over which the conventional correction can be applicable.

Herak and Herak (1993) found new empirical formula for M_S as

$$M_S = \log (A/T)_{\max} + 1,094.\log (\Delta) + 4,429 \quad (2.4)$$

based on an analysis of surface wave magnitudes of 250 selected earthquakes published in the ISC (International Seismological Center) and NEIC (National Earthquake Information Center) catalogues.

To investigate the effect of distance on M_S calculation, Rezapour and Pearce (1998) determined station magnitudes (M_S^{STA}) from ISC Bulletin data using the Prague formula, with a published surface wave magnitude (M_S^{ISC}) from the vertical component recordings. The differences in magnitude values ($M_S^{ISC} - M_S^{STA}$) established for waves of the same type at different stations are mainly due to different conditions at the station, path effects, source effects, and instrumentation. According to Rezapour and Pearce (1998) M_S^{ISC} for larger distances is overestimated, and for closer distances, is underestimated. Confirming the results of Herak and Herak (1993), this result indicated that M_S values obtained by the Prague formula are significantly distance dependent and the numerical value of the constant 1.66 in the Prague formula is too large.

As Herak and Herak have pointed out, M_S^{Prague} values are significantly distance dependent. The mean magnitude obtained by averaging all reported magnitude values is not a representative estimate of the earthquake's strength.

Therefore the modified Prague formula is proposed by Rezapour and Pearce in 1998;

$$M_S^{M.P.} = \log (A/T)_{\max} + 1,555.\log (\Delta) + 4,269 \quad (2.5)$$

In order to compare three different M_S formulae we plotted $\log(\Delta)+\text{constant}$ terms as a function of epicentral distance

(Figure 2.2). The figure indicates that beyond 70° distances Prague formula and Herak and Herak formula gives approximately the same M_S values. On the other hand, Modified Prague formula gives same M_S values in closer ranges with Herak and Herak formula although for both of the other formulae it gives different values in farther ranges.

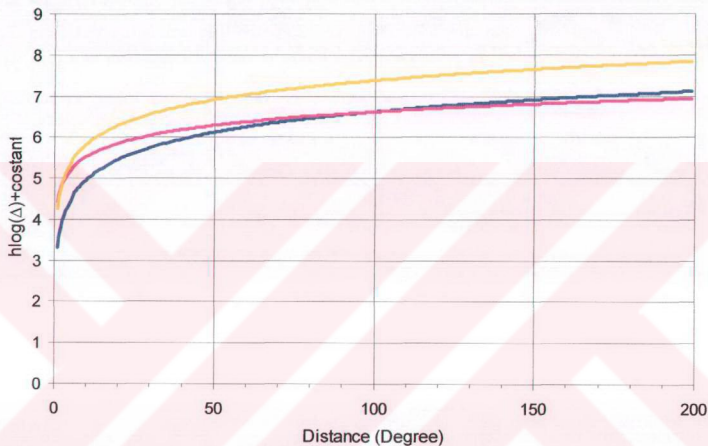


Figure 2.2: " $h\log(\Delta)+\text{constant}$ " term of each formula versus epicentral distance; Prague Formula (blue), Herak and Herak Formula (pink), Modified Prague Formula (yellow).

2.2. DATA

In this study, 25 earthquakes which occurred between the years 1997 and 2004 in and around Turkey were selected for M_S calculation. Selected earthquakes are reported by KOERI (Kandilli Observatory and Earthquake Research Institute), ORFEUS (Observatories and Research Facilities for European Seismology), and IRIS (The Incorporated Research Institutions for Seismology) with M_W (Moment Magnitude) and M_S (Surface Wave Magnitude) values. Earthquakes are listed in Table 2.1. Locations are illustrated in Figure 2.3.

Table 2.1: List of earthquakes used in M_S calculations.

#	Event Origin Time (dd.mn.yy hr:mn)	Location	Latitude (N°)	Longitude (E°)	Depth (km)	M_W	M_S
1	28.02.1997 12:57	IRAN	38.08	48.05	10	6,1	6,1
2	27.06.1998 13:55	TURKEY	36.96	35.52	33	6,3	---
3	06.06.2000 02:41	Çankırı / TURKEY	40.69	32.99	10	6,0	6,1
4	22.08.2000 16:55	IRAN	38.12	57.38	10	5,9	---
5	06.12.2000 17:11	Caspian Sea / INLAND	39.57	54.80	30	7,2	7,5
6	15.12.2000 16:44	Afyon / TURKEY	38.46	31.35	10	6,0	---
7	26.07.2001 00:21	Aegean Sea	39.06	24.24	10	6,3	6,6
8	03.02.2002 07:11	Sultandağ / TURKEY	38.57	31.27	5	6,5	---
9	03.02.2002 09:26	Sultandağ / TURKEY	38.63	30.90	10	6,0	---
10	24.04.2002 19:48	IRAN	34.64	47.40	33	5,4	---
11	25.09.2002 22:28	WESTERN IRAN	32.00	49.33	10	5,6	---
12	27.01.2003 05:26	Pülümür / TURKEY	39.50	39.88	10	6,1	---
13	01.05.2003 00:27	Bingöl / TURKEY	39.01	40.46	10	6,4	6,4
14	06.07.2003 19:10	Saros / TURKEY	40.44	26.13	17	5,8	---
15	13.07.2003 01:48	Pötürge / TURKEY	38.29	38.96	10	5,6	6
16	26.07.2003 08:37	Buldan / Turkey	38.02	28.93	10	5,4	5,6
17	14.08.2003 05:14	GREECE	39.16	20.60	10	6,3	---
18	17.10.2003 12:58	SOUTHERN GREECE	35.94	22.16	33	5,5	---
19	26.12.2003 02:00	SOUTHERN IRAN	29.00	58.31	10	6,5	6,8
20	17.03.2004 05:21	CRETE	34.59	23.33	24	6,1	6
21	25.03.2004 19:30	Erzurum / TURKEY	39.93	40.81	10	5,6	5,5
22	28.05.2004 12:38	IRAN	36.25	51.62	17	6,2	6,4
23	01.07.2004 22:30	Ağrı / TURKEY	39.79	43.88	5	5,1	---
24	04.08.2004 03:01	Bodrum / TURKEY	36.81	27.83	10	5,5	---
25	11.08.2004 15:48	Elazığ / TURKEY	38.34	39.25	7	5,5	---

Waveform data were obtained from IRIS (ORFEUS), KOERI Network Data Archive System (KO), GEOFON (GE), National Observatory of Athens Digital Broadband Network (HL), IRIS/USGS Network (IU), Mediterranean Very Broadband Seismographic Network (MN), Netherlands Seismic Network (NL), and, Israel (IS), Germany (GR), Check Republic (CZ), and Poland (PL) Networks. A total of 72 stations were used for analysis (Table C-1, Appendix C). Each earthquake was recorded by at least 6 or more stations. Sampling rate of the stations is varying from 20 sample/sec to 100 sample/sec. The stations have three component broadband instruments appropriate for M_s calculations.

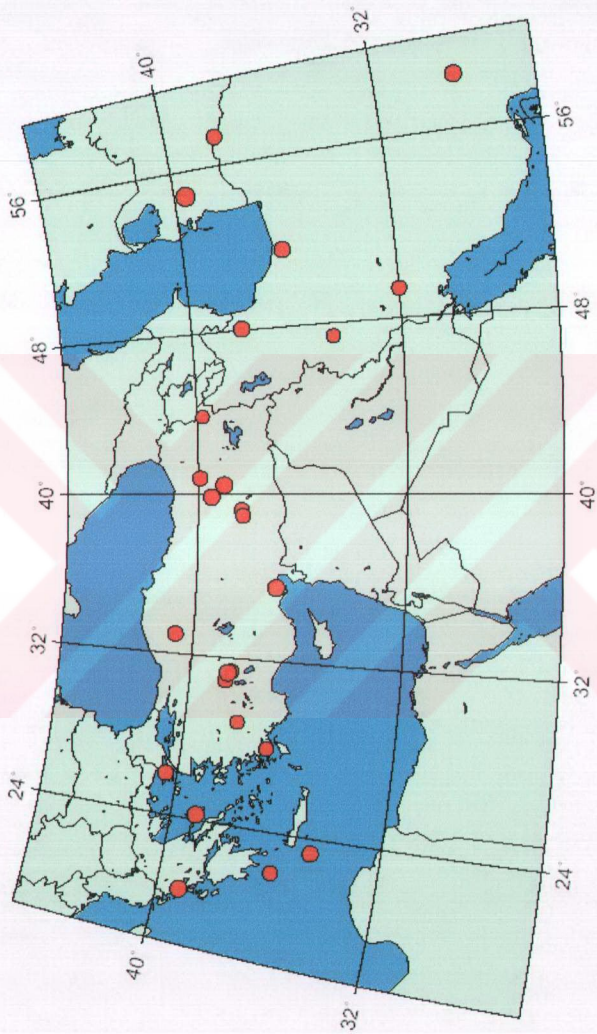


Figure 2.3: The selected earthquakes used in M_s calculations and listed in Table 2.1 which occurred between 1997 and 2004.

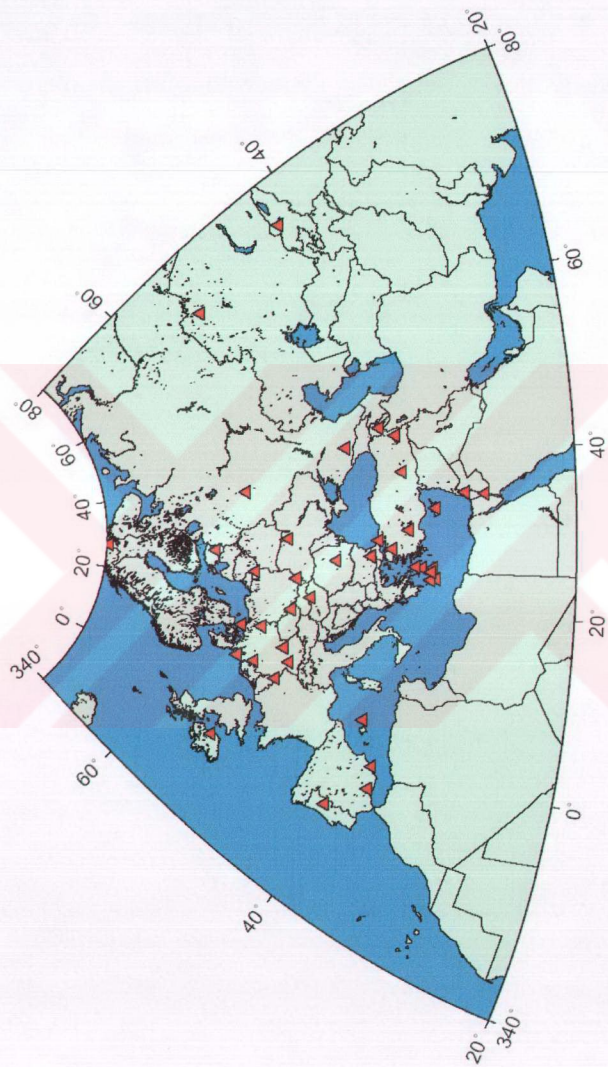


Figure 2.4: The station distribution used in M_s calculation.

The selected events have moment magnitudes between 5.1 and 7.2 and focal depths are less than 60 km. M_S was calculated for stations at distances from 5° to 40° . The data quality was checked and the waveform with low signal/noise ratio was ignored. Using a process outlined in Figure 2.5 surface wave magnitude for each event is calculated.

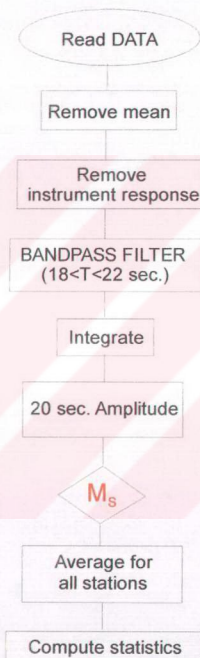


Figure 2.5: Steps in M_S calculation.

Figure 2.5 shows the steps necessary for the surface wave magnitude calculation. The mean of the data was removed in the first step. A bandpass filter of 18-22 sec was used to obtain 20 sec surface waves.

The velocity seismograms was integrated in the frequency domain and converted to displacement seismogram. Instrument response was removed by multiplying the filtered data by a constant which converts velocity seismogram at 20 sec to displacement seismogram. Magnitude is calculated from the maximum amplitude using Prague, Herak and Herak, and Modified Prague formulae listed below

Prague Formula:

$$M_S^{\text{Prague}} = \log (A/T)_{\max} + 1,66.\log (\Delta) + 3,3$$

Herak and Herak Formula:

$$M_S^{\text{H\&H}} = \log (A/T)_{\max} + 1,094.\log (\Delta) + 4,429$$

Modified Prague Formula:

$$M_S^{\text{M.P.}} = \log (A/T)_{\max} + 1,555.\log (\Delta) + 4,269$$

In order to illustrate how M_S magnitude is calculated, we present two examples of an earthquake recorded at two stations. Figure 2.6 shows the vertical component seismogram of Greece Earthquake occurred at 14 August 2003 ($M_W=6.3$) and recorded by ISP station and Figure 2.7 shows the vertical component seismogram of same earthquake recorded by MTE station. The epicentral distance to the ISP (Isparta) station is $\Delta=7.8957^\circ$ and $\Delta=21.6330^\circ$ for MTE station.

Following are the parameters to calculate M_S at ISP station:

ISP Station Scale Factor (S_c) = $1.02906 \cdot 10^{-9}$ (for vertical component)

Maximum amplitude (A_{\max}) = $6,22 \cdot 10^4 \cdot 1,02906 \cdot 10^{-9} \cdot 10^6 = 64,09$ micron

Epicentral distance (Δ) = 7.8957°

Period (T) = 20 sec.

When we do the calculations,

$$M_S^{\text{Prague}} = \log (64.09/20)_{\max} + 1,66.\log (7.8957) + 3,3 = 5.28$$

$$M_S^{\text{H\&H}} = \log (64.09/20)_{\max} + 1,094.\log (7.8957) + 4,429 = 5.91$$

$$M_S^{\text{M.P.}} = \log (64.09/20)_{\max} + 1,555.\log (7.8957) + 4,269 = 6.17$$

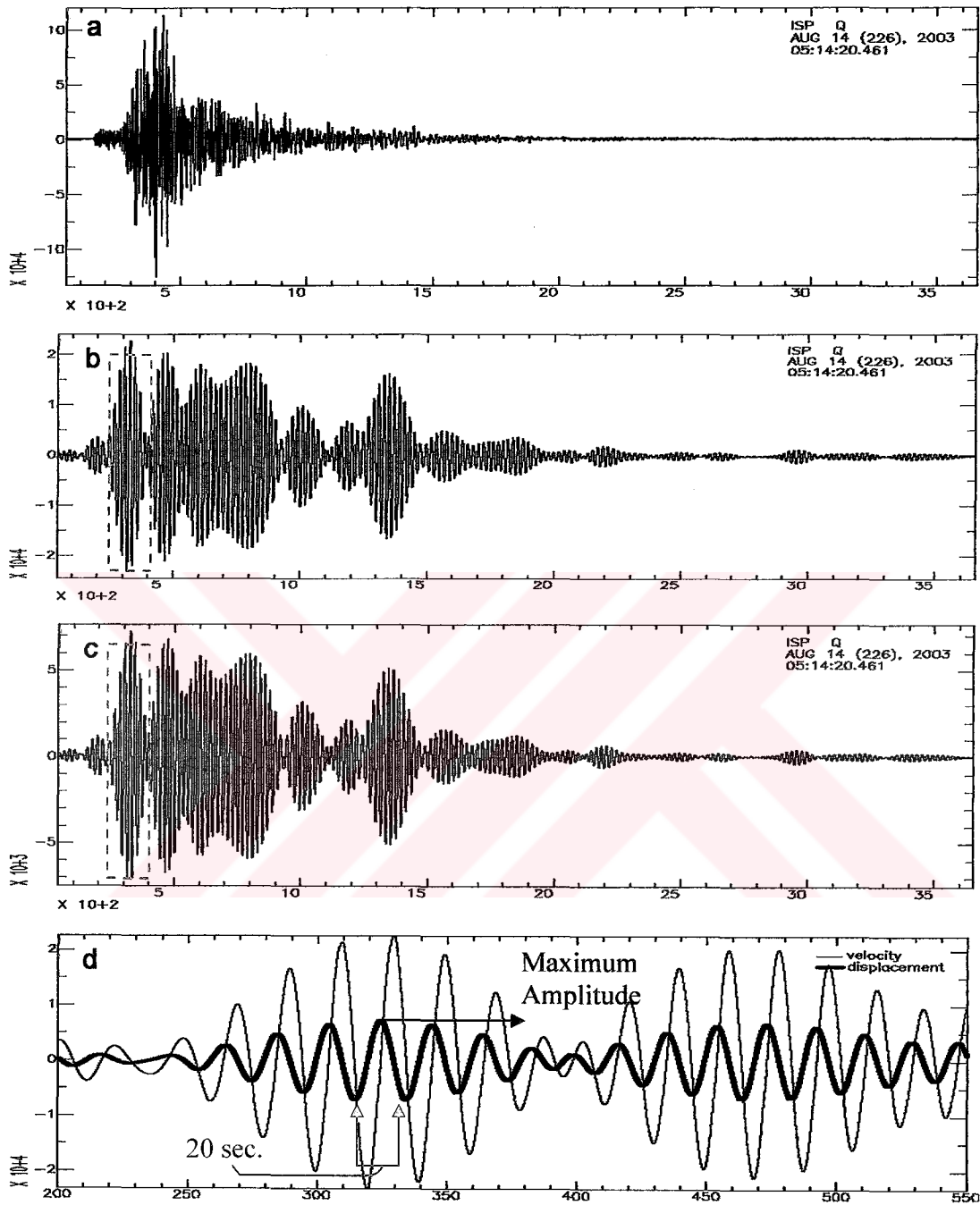


Figure 2.6: a) Vertical component recording of the earthquake occurred in Greece on 14 August 2004 ($M_w=6.3$) recorded at Isparta (ISP) station, b) Filtered with a bandpass filter of 18-22 sec., c) Filtered velocity seismogram converted to displacement, d) Filtered velocity and displacement seismogram in the marked area.

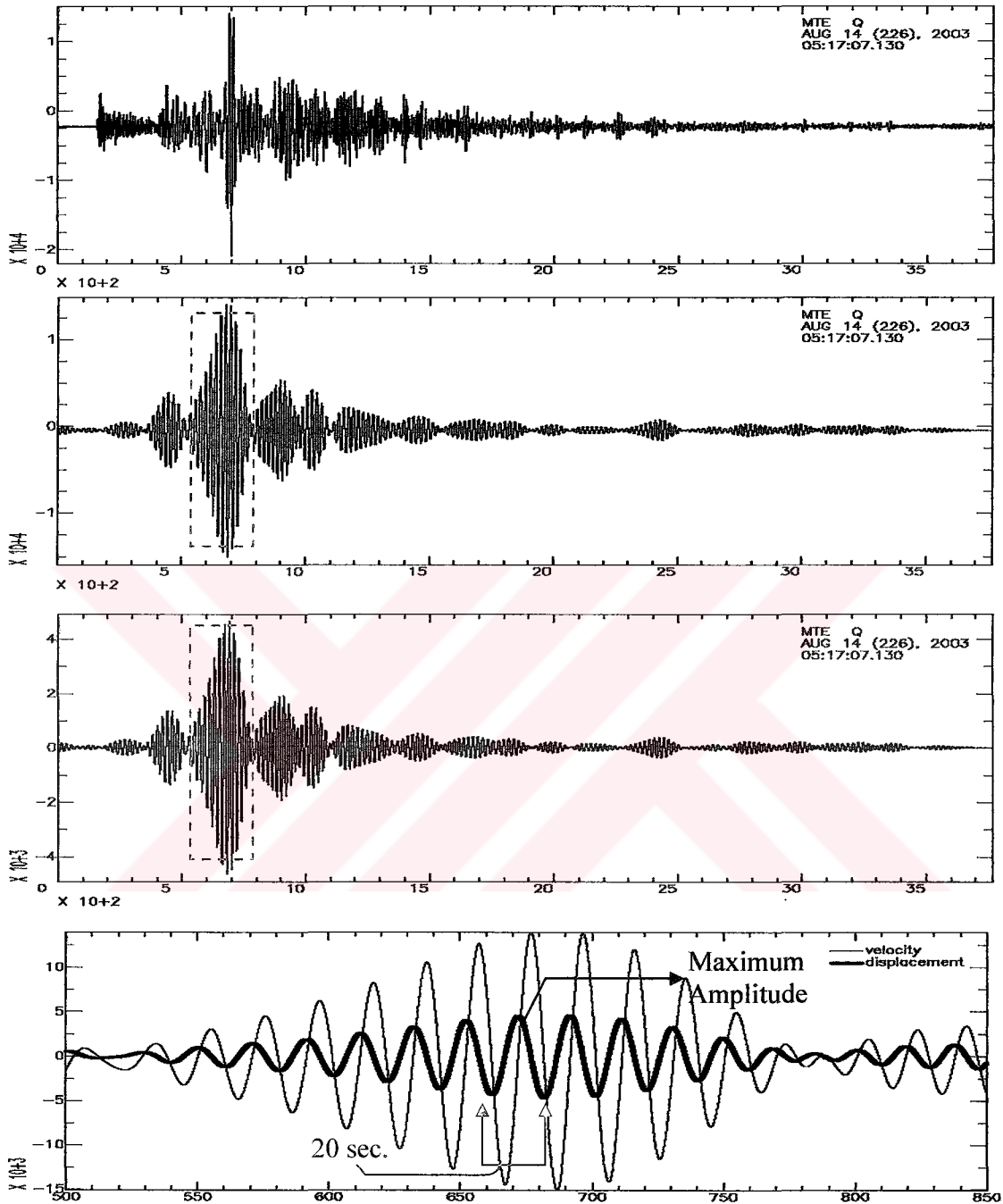


Figure 2.7: a) Vertical component recording of the earthquake occurred in Greece on 14 August 2004 ($M_w=6.3$) recorded at Portugal (MTE) station, b) Filtered with a bandpass filter of 18-22 sec., c) Filtered velocity seismogram converted to displacement, d) Filtered velocity and displacement seismogram in the marked area.

2.3. ANALYSIS & DISCUSSIONS

Table 2.2 shows calculated M_S values with Prague Formula (M_S^{Prague}), Herak and Herak Formula ($M_S^{\text{H\&H}}$) and Modified Prague Formula ($M_S^{\text{M.P.}}$) for 25 regional earthquakes occurred between the years 1997 and 2004. There are significant differences between the magnitudes. Herak and Herak and Modified Prague formulae similar with each other but Prague formula calculations underestimate. In order to understand the origin of these differences it is necessary to investigate the effect of the distance on the magnitude estimation.

Table 2.2: List of M_S values calculated by using different formulae.

#	Event Origin Time (dd.mn.yy hr:mn)	Location	Depth (km)	M_W	M_S	M_S^{Prague}	$M_S^{\text{H\&H}}$	$M_S^{\text{M.P.}}$
1	28.02.1997 12:57	IRAN	10	6,1	6,1	5.8	6.3	6.7
2	27.06.1998 13:55	TURKEY	33	6,3	—	5.8	6.1	6.6
3	06.06.2000 02:41	Çankırı / TURKEY	10	6,0	6,1	5.5	6.0	6.3
4	22.08.2000 16:55	IRAN	10	5,9	—	5.2	5.5	6.0
5	06.12.2000 17:11	Caspian Sea / INLAND	30	7,2	7,5	6.7	7.0	7.5
6	15.12.2000 16:44	Afyon / TURKEY	10	6,0	—	5.3	5.9	6.2
7	26.07.2001 00:21	Aegean Sea	10	6,3	6,6	6.2	6.6	7.0
8	03.02.2002 07:11	Sultandağ / TURKEY	5	6,5	—	6.0	6.5	6.8
9	03.02.2002 09:26	Sultandağ / TURKEY	10	6,0	—	5.3	5.8	6.2
10	24.04.2002 19:48	IRAN	33	5,4	—	5.5	5.8	6.3
11	25.09.2002 22:28	WESTERN IRAN	10	5,6	—	4.8	5.3	5.7
12	27.01.2003 05:26	Pülümür / TURKEY	10	6,1	—	5.7	6.1	6.5
13	01.05.2003 00:27	Bingöl / TURKEY	10	6,4	6,4	6.0	6.3	6.8
14	06.07.2003 19:10	Saros / TURKEY	17	5,8	—	5.0	5.5	5.8
15	13.07.2003 01:48	Pötürge /TURKEY	10	5,6	6	4.9	5.5	5.8
16	26.07.2003 08:37	Buldan / Turkey	10	5,4	5,6	4.8	5.2	5.6
17	14.08.2003 05:14	GREECE	10	6,3	—	5.8	6.3	6.6
18	17.10.2003 12:58	SOUTHERN GREECE	33	5,5	—	4.9	5.5	5.8
19	26.12.2003 02:00	SOUTHERN IRAN	10	6,5	6,8	6.5	6.8	6.7
20	17.03.2004 05:21	CRETE	24	6,1	6	5.2	5.7	6.0
21	25.03.2004 19:30	Erzurum / TURKEY	10	5,6	5,5	4.9	5.4	5.7
22	28.05.2004 12:38	IRAN	17	6,2	6,4	6.2	6.6	7.0
23	01.07.2004 22:30	Ağrı / TURKEY	5	5,1	—	4.3	4.7	5.2
24	04.08.2004 03:01	Bodrum / TURKEY	10	5,5	—	4.8	5.2	5.1
25	11.08.2004 15:48	Elazığ / TURKEY	7	5,5	—	5.2	5.7	6.1

Figure 2.8 shows the M_s estimates for the Bingöl Earthquake ($M_w=6.4$) at distances from 5 to 40 degrees. Average M_s value for Prague formula is 6.0, 6.3 for Herak and Herak and 6.8 for Modified Prague. The results of Prague formula, Herak and Herak formula and Modified Prague formula for different seismic stations at different distance ranges are shown. The Prague formula underestimates the magnitude while modified Prague formula overestimates. The Herak and Herak formula is in better agreement with $M_w=6.4$. There is dependency on the distance for all three formulae.

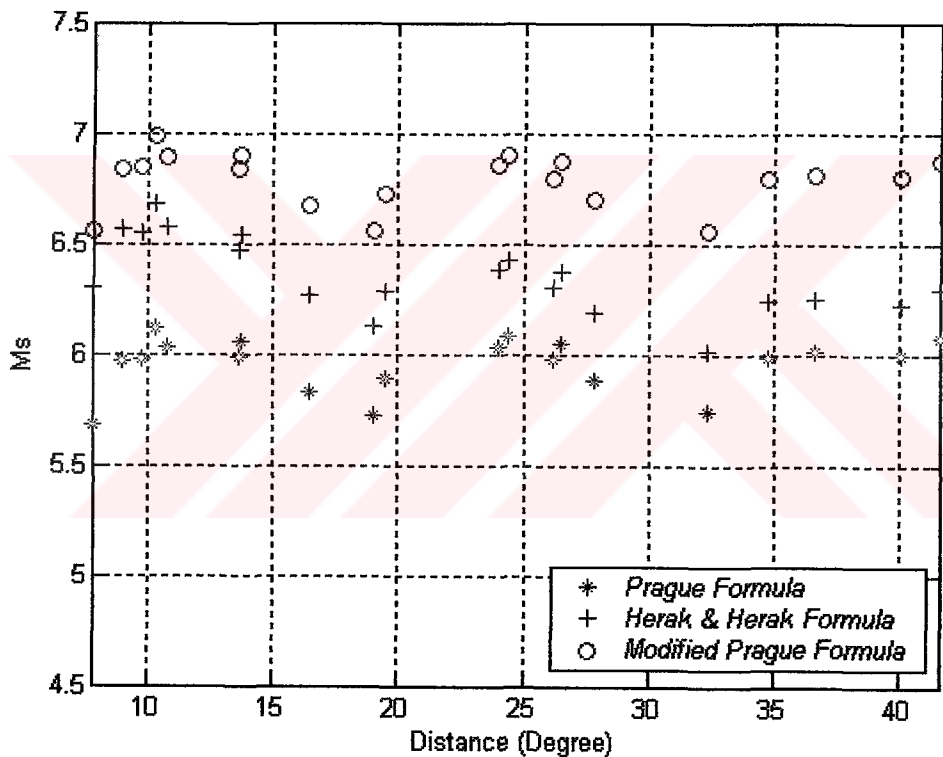


Figure 2.8: M_s values of the Bingöl ($M_w=6.4$) earthquake as a function of epicentral distance.

In order to reach a more meaningful conclusion, we need to examine the M_s magnitudes from all earthquakes as a function of distance. Figures 2.9-2.11 illustrates the deviations from the average M_s values, for 25 earthquakes, as a function of distance. The Prague formula and

Modified Prague formula show dependency to epicentral distance while the Herak and Herak formula does not show any significant dependency. It is also worthwhile to mention that the deviation from the average M_s values is around 0.3 for Prague formula and for Modified Prague formula. As shown in Figure 2.2 (Section 2.1.1), Prague formula and Modified Prague formula has almost same characteristics while Herak and Herak has not. So it is expected that both the Prague and Modified Prague formulae acts similar while Herak and Herak not.

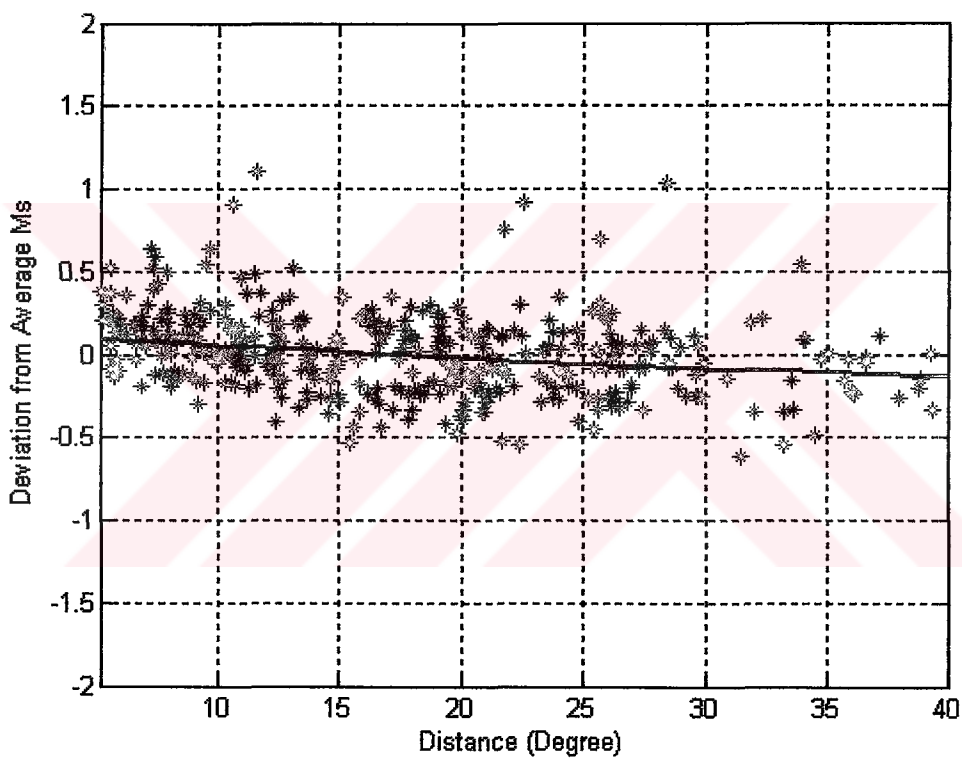


Figure 2.9: Surface wave magnitudes deviation from average M_s values as a function of epicentral distance using the Prague Formula. The blue line represents the least square fit.

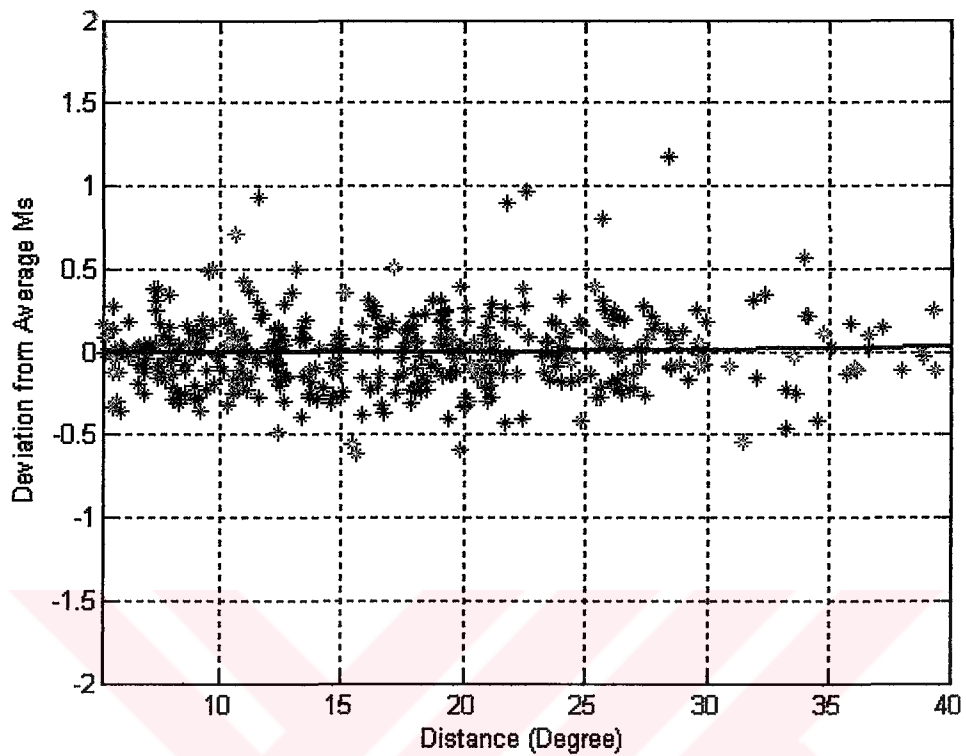


Figure 2.10: Surface wave magnitudes deviation from average M_s values as a function of epicentral distance using the Herak and Herak Formula. The blue line represents the least square fit.

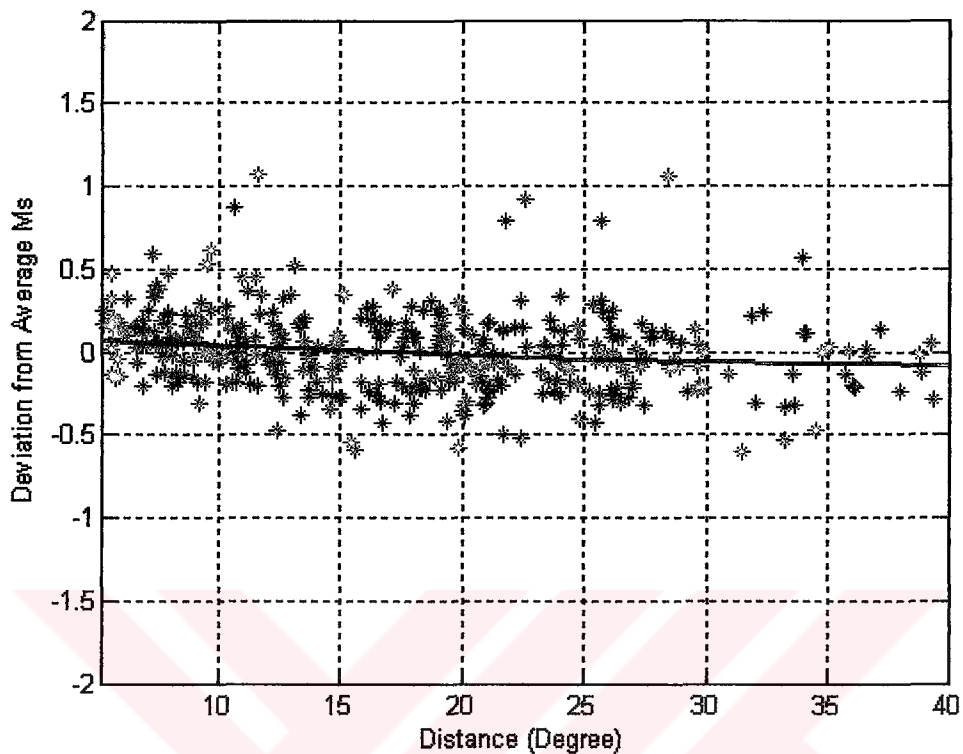


Figure 2.11: Surface wave magnitudes deviation from average M_s values as a function of epicentral distance using the Modified Prague Formula. The blue line represents the least square fit.

In addition to the analysis above, it was important to discuss the correlation between surface wave magnitude (M_s) and moment magnitude (M_w). We ignored the biases in the moment magnitudes which were obtained from different sources. Figure 2.12 shows the correlation between M_s and M_w for three M_s formulae. The calculated M_s magnitudes by using Prague formula are lower than the M_w magnitudes. On the other hand surface wave magnitudes calculated by using Modified Prague formula are higher than the M_w values. However the Herak and Herak formula has better correlation with M_w .

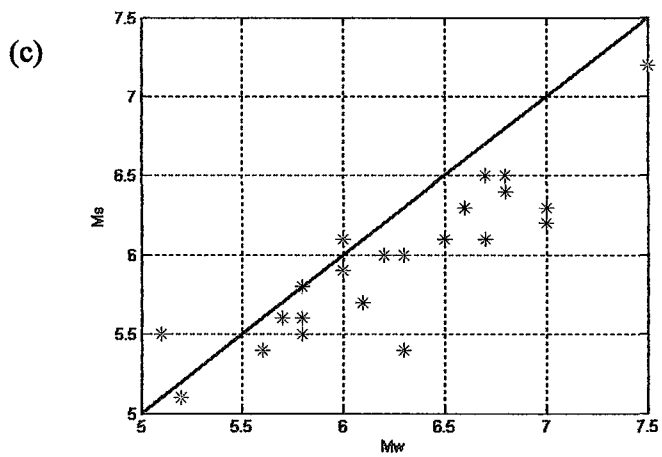
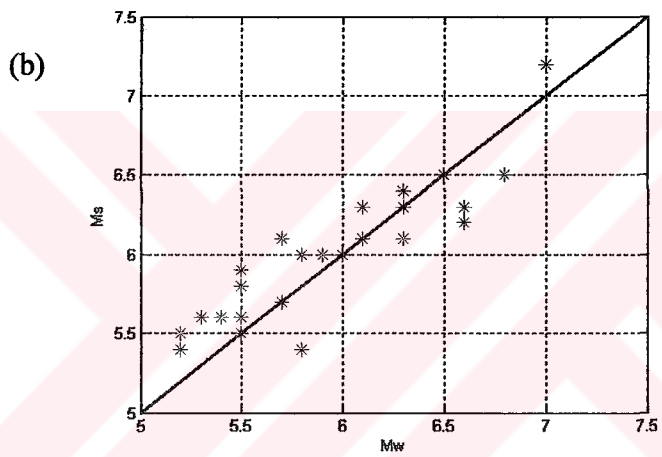
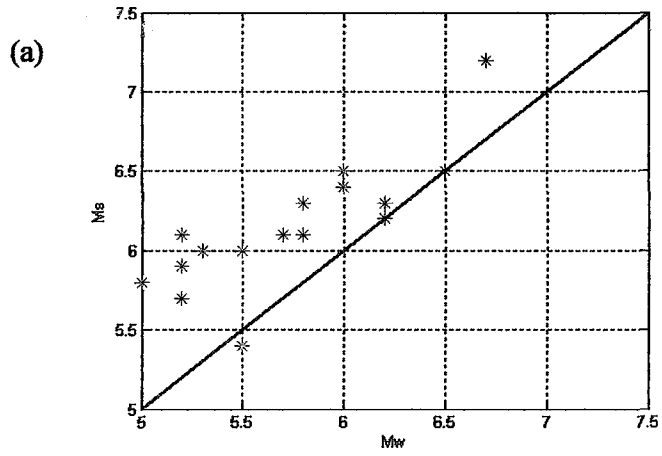


Figure 2.12: M_w versus M_s for Prague Formula (a), Herak and Herak Formula (b), Modified Prague Formula (c).

2.4. CONCLUSION

The surface wave magnitudes (M_S) of 25 earthquakes which occurred in and around Turkey was calculated by using the Prague, Herak and Herak and Modified Prague formulae. The surface wave magnitudes (M_S) are compared with moment magnitudes (M_W).

The Prague Formula is inappropriate for magnitude determination at distances less than 20 degree since it produces significant distance-dependent estimates. The average difference between M_S values at small epicentral distances and those at large distances exceed 0.3 magnitude units, so it prevents the use of magnitudes for seismicity and related studies.

In the Herak and Herak Formula the average difference between M_S values at close epicentral distances and those at large distances exceed less than 0.1 magnitude units while M_S values are more stable for Modified Prague formula calculated by Rezapour and Pearce (1998). On the other hand, in an investigation of the distance dependency, we conclude that in Herak and Herak formula, the residuals of individual station magnitudes from the mean magnitudes are less than in other formulae.

In comparing M_W and M_S estimates, Prague Formula and Modified Prague Formula have significantly different M_S values from the M_W values. Herak and Herak formula has better correlation with the M_W values.

As a result, we propose that, Herak and Herak formula is the most reasonable formula to be used to calculate M_S values of regional earthquakes occurring in and around Turkey.

REFERENCES

- Aki, K., Richards, P. G., 1980. Quantitative Seismology: Theory and Methods, W.H.Freeman, San Francisco.
- Basham, P.W. 1971. A new magnitude formula for short-period continental Rayleigh waves, *Geophys. J. R. Ast. Soc.*, 23, 255.
- Bath, M., 1966. Earthquake energy and magnitude, *Phys. & Chem. of the earth*, 7, 115-165.
- Christoskov, L. 1965. Magnitude-dependent calibrating functions of surface waves for Sofia, *Studia Geoph. et Geod.*, 9, 331-340.
- Crosson, R.S., 1976. Crustal structure modeling of earthquake data 1. simultaneous least square estimation of hypocenter and velocity parameters, *J. Geophys. Res.*, 17, 1976.
- Çağatay, M.N., Görür, N., Alpar, B., Saatçılar, R., Akkök, R., Sakiñç, M., Yüce, H., Yaltırak, C., Kuşçu, İ., 1998. Geological evolution of the Gulf of Saros, NE Aegean, *Geo-Mar. Lett.* 18, 1-9.
- Evernden, J.F., 1971. Variation of Rayleigh-wave amplitude with distance, *Bull. Seism. Soc. Am.* 61, 231-240.
- Gutenberg, B., 1945. Amplitudes of surface waves and magnitudes of shallow earthquakes, *Bull. Seism. Soc. Am.* 35, 3-12.
- Gutenberg, B., Richter, C., 1942. Earthquake magnitude, intensity, energy and acceleration, *Bull. Seism. Soc. Am.*, 32, 163-191.
- Herak, M., Herak, D., 1993. Distance dependence of M_S and calibrating function for 20 second Rayleigh waves, *Bull. Seism. Soc. Am.* 83, 1881-1892.
- Kissling, E., Ellsworth, W.L., Eberhart-Philips, D., Kradolfer, U., 1994. Initial reference models in local earthquake tomography, *J. Geophys. Res.*, 99, 19,635-19,646.
- Kurt, H., Demirbağ, E., Kuşçu, İ., 2000. Active submarine tectonism and formation of the Gulf of Saros, NE Aegean Sea, inferred from

- multi-channel seismic reflection data, *Marine Geology* 165, 13-26.
- Le Pichon, X., Şengör, A.M.C., Demirbağ, E., Rangin, C., İmren, C., Armijo, R., Görür, N., Çağatay, N., Mercier de Lepinay, B., Meyer, B., Saatçılar, R., Tok, B., 2001. The active main Marmara fault, earth and planetary, *Science Letters* 192, 595-616.
- Lienert, B.R., 1994. HYPOCENTER 3.2, A Computer Program for Locating Earthquakes Locally, Regionally and Globally User's Manual.
- Marshall, P.D., Basham, P.W., 1972. Discrimination between earthquakes and underground explosions employing an improved M_S scale, *Geophys. J. R. Astr. Soc.*, 29, 431-458.
- Okal, E.A., 1989. A theoretical discussion of time domain magnitude: the Prague formula for M_S and the mantle magnitude M_M , *J. Geophys. Res.* 94, 4194-4204.
- Özalaybey, S., Ergin, M., Aktar, M., Tapırdamaz, C., Biçmen, F., Yörük, A., 2002. The 1999 Izmit earthquake sequence in Turkey: Seismological and tectonic aspects, *Bull. Seism. Soc. Am.* 92, 376-386.
- Prozorov, A., Hudson, J.A., 1974. A study of the magnitude difference M_S-M_b for earthquakes, *Geophys. J. R. Astr. Soc.* 39, 551-564.
- Reasanberg, P. A., and D. H. Oppenheimer 1985. FPFIT, FPLOT, and FPPAGE: Fortran computer programs for calculating and displaying earthquake fault-plane solutions, *U.S. Geol. Surv. Open-File Rept.* 109, 85-739.
- Rezapour, M., Pearce, R.G., 1998. Bias in surface-wave magnitude M_S due to inadequate distance corrections, *Bull. Seism. Soc. Am.* 88, 43-61.
- Richter, C., 1935. An instrumental earthquake magnitude scale, *Bull. Seism. Soc. Am.*, 25, 1-32.

- Saatçılar, R., Ergintav, S., Demirbağ, E., Inan, S., 1999. Character of active faulting in the Northern Aegean Sea, *Mar. Geol.* 160, 339-353.
- Soloviev, S. L. 1955. O klassifikatsiy zemletrayaseniy po velichine ikh energii (Classification of earthquakes in order of energy), *Trudy Geofiz. Inst. AN SSSR*, 30, 3-31.
- Soloviev, S. L., Shebalin, N. V., 1957. Opredelenie intensivnosti zemletryaseniya po smeshcheniyu pochvy v poverkhnostnykh (Determination of intensity of earthquakes according to ground displacements in the surface waves), *Izv. AN SSSR, ser. geofiz.*, 7, 926-930.
- Thomas, J.H., Marshall P.D., Douglas A., 1978. Rayleigh-wave amplitudes from earthquakes in the range of 0°-150°, *Geophys. J. R. Astr. Soc.* 53, 191-200.
- Vanek, J., Stelzner, J., 1959. Bestimmung der Magnitudengleichen für Jena (Determination of the magnitude function for Jena), *Gerl. Beitr. zu Geophys.*, 77, 105-119.
- Vanek, J., A. Zatopek, V. Karnik, Y.V. Riznichenko, E.F. Saverensky, S.L. Soloviev, and N.V. Shebalin 1962. Standardization of magnitude scales, *Bull. (Izvest.) Acad. Sci. U.S.S.R., Geophys. Ser.*, 2, 108.
- von Seggern, D.H., 1977. Amplitude-distance relation for 20 second Rayleigh waves, *Bull. Seism. Soc. Am.* 67, 405-411.

APPENDIX A

Table A-1: List of seismic stations and coordinates used for Saros earthquake sequence analysis. IU: IRIS/USGS Network, HL: National Observatory of Athens Digital Broadband Network, TK: TÜBITAK, Marmara Research Center, GE: GEOFON Network, KO: Kandilli Observatory and Earthquake Research Institute Network.

Station Name	Network Code	Latitude (N°)	Longitude (E°)	Elevation (m)	Location
AGG	-	3901.32	2219.80	-	-
AKS	KO	3852.77	2748.80	370	Turkey
ALN	-	4053.10	2602.76	-	-
ALT	KO	3903.31	3006.62	1050	Turkey
AMT	KO	4033.57	2851.41	428	Turkey
ANTO	IU	3952.13	3247.62	883	Turkey
AOS	-	3910.20	2352.80	-	-
APE	GE	3704.13	2531.84	620	Greece
ARG	HL	3613.20	2807.80	170	Greece
ATH	HL	3758.20	2343.20	-	-
AVC	TK	4104.86	2841.64	50	Turkey
BALB	KO	3938.40	2752.80	-	Turkey
BNT	KO	4021.36	2755.20	353	Turkey
CAN	KO	4036.37	3337.18	815	Turkey
CEV	TK	4022.14	2634.98	50	Turkey
CEY	KO	3700.64	3544.87	100	Turkey
CTT	KO	4108.84	2825.78	324	Turkey
DEN	KO	3745.22	2901.99	637	Turkey
DST	KO	3936.24	2837.15	625	Turkey
EDC	KO	4020.81	2751.80	269	Turkey
EDRB	KO	4150.82	2644.62	-	Turkey
ELL	KO	3644.90	2954.51	1230	Turkey
ERZ	KO	3945.12	3921.20	1500	Turkey
ESK	KO	3931.33	3050.98	1289	Turkey
EVR	HL	3855.20	2148.60	-	-
EZN	KO	3949.55	2619.52	49	Turkey
FNA	-	4047.04	2122.92	-	-
GAZ	KO	3710.33	3712.68	864	Turkey
GPA	KO	4017.09	3019.02	572	Turkey
GRG	-	4057.42	2224.06	-	-
HDMB	KO	3657.84	3229.16	1946	Turkey
HRT	KO	4049.30	2940.08	645	Turkey
HRTX	KO	4049.30	2940.08	645	Turkey

IBBN	GE	5218.43	0745.40	140	Germany
IKL	KO	3614.32	3341.11	120	Turkey
ISKB	KO	4103.94	2903.55	132	Turkey
ISP	GE	3749.36	3031.33	1000	Turkey
ITM	HL	3710.80	2155.80	400	Greece
IZI	KO	4020.21	2928.37	910	Turkey
IZM	KO	3823.87	2715.75	631	Turkey
JAN	HL	3939.60	2051.00	-	-
KAM	KO	3922.15	3342.76	-	Turkey
KAP	HL	3533.00	2710.80	-	-
KAR	-	4028.86	2904.26	122	-
KCT	KO	4015.93	2821.39	451	Turkey
KEK	HL	3942.60	1948.00	280	Greece
KGT	KO	4027.09	2718.20	185	Turkey
KGZ	-	4101.62	2821.15	50	-
KHL	KO	3819.39	2931.39	940	Turkey
KIZ	KO	3852.90	3153.00	1202	Turkey
KNL	TK	4016.20	2731.56	30	Turkey
KON	KO	3756.72	3221.63	1100	Turkey
KZN	HL	4018.60	2146.20	-	-
LAP	KO	4022.36	2645.61	200	Turkey
LIA	HL	3954.00	2510.80	-	-
LIT	-	4006.06	2229.40	-	-
LKR	HL	3839.00	2300.00	-	-
LOS	-	3955.98	2504.86	-	-
MAD	-	4039.21	2739.88	-	-
MALT	GE	3818.78	3825.62	-	Turkey
MAR	-	4058.02	2757.66	50	-
MEV	-	3947.10	2113.74	1500	-
MFT	KO	4047.28	2718.04	924	Turkey
MFTX	KO	4047.28	2718.04	924	Turkey
MLR	-	4529.42	2556.74	-	-
MLSB	KO	3718.60	2747.40	500	Turkey
MORC	GE	4946.60	1732.57	740	Czech Rep.
MRMX	KO	4036.54	2734.98	702	Turkey
MTE	GE	4023.98	-0732.65	-	Portugal
MUD	KO	4027.92	3112.87	-	Turkey
NEO	HL	3918.60	2313.20	-	-
NIG	KO	3806.53	3436.87	2291	Turkey
NPS	HL	3515.60	2536.60	-	-
NVR	HL	4121.00	2351.60	-	-
ORC	-	4042.28	2947.34	80	-
ORL	KO	4002.77	2853.75	649	Turkey
OUR	-	4020.04	2358.92	-	-
PAIG	-	3955.62	2340.80	-	-
PLG	HL	4022.20	2327.00	-	-

PRK	HL	3913.80	2616.20	-	-
PVL	-	4051.42	2915.96	10	-
RDO	HL	4109.00	2532.40	100	Greece
RLS	-	3803.60	2128.20	-	-
SAF	KO	4114.39	3241.23	406	Turkey
SGT	-	4046.02	2706.48	50	-
SKD	GE	3524.72	2355.68	306	Greece
SMG	HL	3742.60	2650.40	-	-
SOH	-	4049.32	2321.24	-	-
SRS	-	4107.02	2335.52	-	-
STU	GR	4846.31	0911.70	360	Germany
SUW	PL	5405.50	2310.48	152	Poland
THE	-	4037.92	2257.90	-	-
TOS	KO	4102.17	3401.35	1046	Turkey
TRN	TK	4030.30	2746.68	80	Turkey
VAM	HL	3524.60	2412.00	-	-
VLI	HL	3643.20	2257.00	-	-
VLS	HL	3810.80	2035.40	-	-
YLVX	KO	4034.00	2922.37	829	Turkey

Table A-2: List of seismic stations with corrections used for Saros earthquake sequence analysis.

Station Name	Network Code	Latitude (N°)	Longitude (E°)	Elevation (m)	Location	Station Correction
APE	GE	3704.13	2531.84	620	Greece	0.33
AVC	TK	4104.86	2841.64	50	Turkey	0.24
BALB	KO	3938.40	2752.80	-	Turkey	0.28
BNT	KO	4021.36	2755.20	353	Turkey	0.22
CTT	KO	4108.84	2825.78	324	Turkey	0.12
EDC	KO	4020.81	2751.80	269	Turkey	0.32
EDRB	KO	4150.82	2644.62	-	Turkey	0.14
EZN	KO	3949.55	2619.52	49	Turkey	-0.16
IZM	KO	3823.87	2715.75	631	Turkey	0.65
KNL	TK	4016.20	2731.56	30	Turkey	0.13
LAP	KO	4022.36	2645.61	200	Turkey	-0.10
LIA	HL	3954.00	2510.80	-	-	0.01
MFTX	KO	4047.28	2718.04	924	Turkey	-0.05
MRMX	KO	4036.54	2734.98	702	Turkey	0.01
NVR	HL	4121.00	2351.60	-	-	0.39
PRK	HL	3913.80	2616.20	-	-	0.19
RDO	HL	4109.00	2532.40	100	Greece	-0.20
SMG	HL	3742.60	2650.40	-	-	0.56
TRN	TK	4030.30	2746.68	80	Turkey	0.64

Table A-3: List of Earthquakes located in the Gulf of Saros.

#	Event Origin Time (yr.mn.dd hr:mn:sc.ms)	Latitude (N°)	Longitude (E°)	Depth (km)	Magnitude M _L
1	2003.07.05 21:58:29.60	40.441	26.063	11.7	4.3
2	2003.07.06 19:10:28.00	40.427	26.103	17.5	5.8
3	2003.07.06 19:24:51.40	40.448	26.131	17.6	3.6
4	2003.07.06 19:26:22.00	40.428	25.977	11.3	3.6
5	2003.07.06 19:39:50.70	40.411	25.996	18.5	4.2
6	2003.07.06 19:41:08.40	40.411	26.098	15.5	3.6
7	2003.07.06 19:58:37.50	40.407	26.165	19.1	2.8
8	2003.07.06 20:02:44.70	40.430	26.120	17.6	3.4
9	2003.07.06 20:10 15.60	40.439	26.108	16.4	5.3
10	2003.07.06 20:15:52.20	40.429	26.144	16.1	3.3
11	2003.07.06 20:19:53.90	40.431	26.116	17.8	3.2
12	2003.07.06 20:24:18.50	40.381	25.929	8.4	2.8
13	2003.07.06 20:26 42.50	40.405	25.964	10.0	3.3
14	2003.07.06 20:29:49.20	40.362	25.977	11.1	2.8
15	2003.07.06 20:32:06.20	40.370	25.971	15.0	2.8
16	2003.07.06 20:48:53.30	40.406	26.006	19.6	4.7
17	2003.07.06 22:05:48.50	40.403	25.989	16.3	4.2
18	2003.07.06 22:20:31.40	40.362	25.972	11.3	2.6
19	2003.07.06 22:42:08.70	40.405	25.940	13.3	4.4
20	2003.07.06 22:46:04.20	40.399	25.968	10.4	3.0
21	2003.07.06 22:52:09.00	40.434	26.122	8.2	2.3
22	2003.07.06 23:27:19.10	40.369	25.987	12.9	2.3
23	2003.07.06 23:30:21.20	40.398	26.015	14.4	2.6
24	2003.07.06 23:47:20.10	40.358	26.001	13.9	2.6
25	2003.07.06 23:54:54.30	40.394	25.967	13.7	3.2
26	2003.07.07 00:24:07.30	40.381	25.921	9.5	3.4
27	2003.07.07 00:48:15.20	40.393	25.967	13.8	3.5
28	2003.07.07 00:55:35.10	40.410	26.013	9.9	2.7
29	2003.07.07 01:13:13.40	40.420	26.128	15.3	2.3
30	2003.07.07 01:36:39.60	40.392	25.945	10.9	2.7
31	2003.07.07 03:05:43.50	40.392	26.036	17.0	2.8
32	2003.07.07 03:16:25.30	40.382	26.056	17.9	2.4
33	2003.07.07 04:24:07.40	40.412	25.980	6.5	2.4
34	2003.07.07 07:10:11.60	40.433	26.068	14.9	2.6
35	2003.07.07 07:12:02.50	40.383	25.924	12.8	3.4
36	2003.07.07 07:15:02.70	40.381	25.881	9.7	3.1
37	2003.07.07 09:59:11.00	40.392	26.158	17.0	2.5
38	2003.07.07 10:45:48.60	40.409	26.159	12.4	3.0
39	2003.07.07 12:49:32.20	40.431	26.193	16.2	2.9

40	2003.07.07 14:08:02.00	40.403	26.031	13.0	2.8
41	2003.07.07 14:30:56.60	40.417	26.206	11.5	2.2
42	2003.07.07 15:16:49.10	40.401	26.188	7.4	2.6
43	2003.07.07 16:17:38.70	40.403	25.921	12.7	3.4
44	2003.07.07 16:44:02.10	40.398	26.182	17.8	3.0
45	2003.07.07 16:45:40.30	40.386	25.925	13.1	3.4
46	2003.07.07 16:47:41.80	40.363	26.140	15.0	2.7
47	2003.07.07 16:53:39.30	40.399	26.186	18.1	2.7
48	2003.07.07 18:50:29.10	40.371	25.928	10.9	2.7
49	2003.07.07 19:57:45.30	40.396	25.897	10.7	3.3
50	2003.07.07 21:18:28.00	40.400	26.021	14.8	2.7
51	2003.07.07 21:41:13.20	40.416	26.177	15.0	2.4
52	2003.07.07 23:28:19.40	40.436	26.134	13.5	2.6
53	2003.07.07 23:44:30.30	40.410	26.093	12.6	2.5
54	2003.07.08 01:24:45.10	40.397	25.957	10.6	2.6
55	2003.07.08 04:31:23.80	40.411	26.177	15.4	3.3
56	2003.07.08 07:28:56.00	40.430	26.201	15.8	2.6
57	2003.07.08 10:12:31.50	40.447	26.056	8.3	2.5
58	2003.07.08 10:14:53.70	40.402	26.006	14.5	3.0
59	2003.07.08 17:20:54.60	40.418	26.232	13.6	2.3
60	2003.07.08 19:29:36.30	40.429	26.218	14.0	2.5
61	2003.07.08 20:51:23.20	40.397	26.072	18.2	2.4
62	2003.07.08 23:42:27.50	40.416	26.175	17.2	3.1
63	2003.07.09 00:06:51.10	40.389	25.940	9.4	2.4
64	2003.07.09 00:07:58.20	40.400	25.920	10.3	3.4
65	2003.07.09 00:21:16.00	40.391	26.165	17.9	2.6
66	2003.07.09 00:23:06.60	40.387	25.916	10.2	2.9
67	2003.07.09 20:51:31.60	40.440	26.158	15.5	2.8
68	2003.07.09 22:01:57.50	40.385	25.913	12.6	3.8
69	2003.07.09 22:08:49.50	40.386	25.902	11.9	4.1
70	2003.07.09 22:31:40.70	40.388	25.912	15.8	4.7
71	2003.07.09 22:37:08.60	40.370	25.882	9.5	3.4
72	2003.07.10 00:05:04.00	40.368	25.913	11.9	3.0
73	2003.07.10 01:26:17.70	40.387	25.912	16.5	4.4
74	2003.07.10 07:33:45.80	40.365	25.902	10.6	2.4
75	2003.07.10 09:01:17.80	40.183	25.305	20.7	4.0
76	2003.07.10 13:25:33.40	40.381	25.897	10.2	3.4
77	2003.07.10 15:10:28.90	40.435	26.162	10.7	2.1
78	2003.07.10 20:14:45.80	40.386	25.893	10.1	3.1
79	2003.07.10 20:30:52.20	40.383	25.863	9.3	2.9
80	2003.07.11 02:56:27.70	40.388	25.849	9.0	2.7
81	2003.07.11 07:22:48.70	40.421	26.165	15.3	3.2
82	2003.07.11 23:51:14.30	40.191	25.283	21.0	3.8

83	2003.07.13 02:06:40.30	40.395	26.135	11.9	2.9
84	2003.07.13 06:20:15.80	40.397	25.921	10.8	3.0
85	2003.07.13 06:32:08.10	40.389	25.923	13.9	4.0
86	2003.07.13 10:12:50.80	40.431	26.064	18.1	3.0
87	2003.07.15 21:49:38.90	40.396	26.145	10.5	3.0
88	2003.07.16 16:24:39.80	40.180	25.293	19.3	3.5
89	2003.07.18 05:44:07.20	40.394	25.962	14.0	3.8
90	2003.07.18 12:52:12.20	40.436	26.116	18.7	3.3
91	2003.07.23 19:37:06.00	40.437	26.153	16.8	2.8
92	2003.08.05 03:48:44.50	40.431	25.984	6.9	2.8
93	2003.08.11 23:14:30.70	40.407	26.256	14.0	2.5
94	2003.08.31 07:50:56.70	40.415	25.972	17.0	4.0
95	2003.09.14 09:15:26.70	40.365	25.980	13.1	2.8
96	2004.06.15 12:02:38.50	40.373	25.901	12.9	5.1

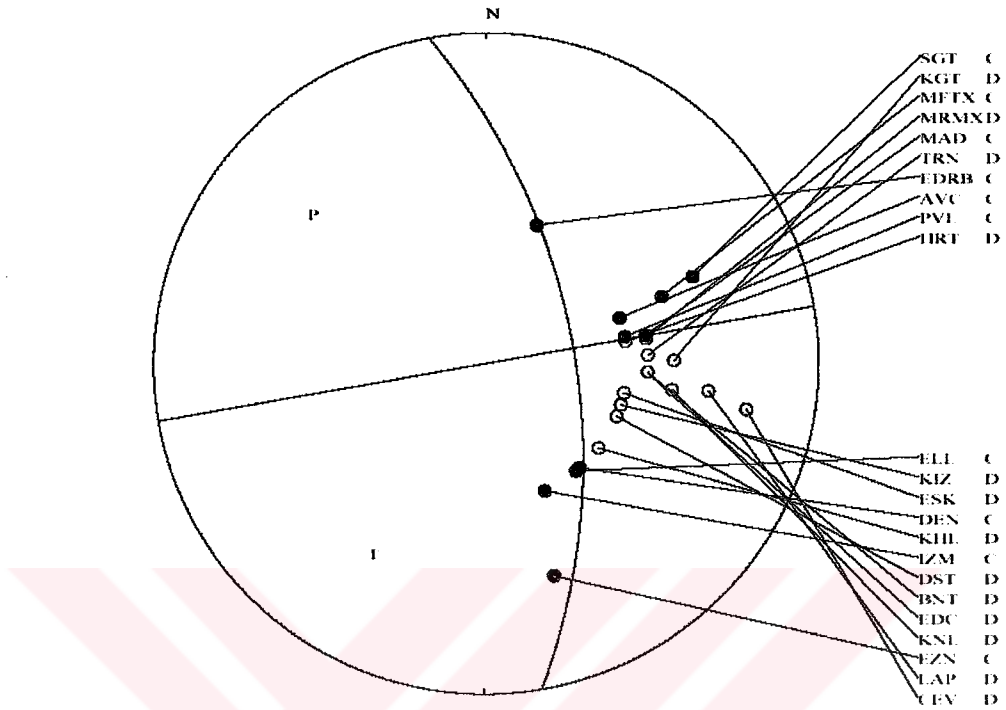


APPENDIX B

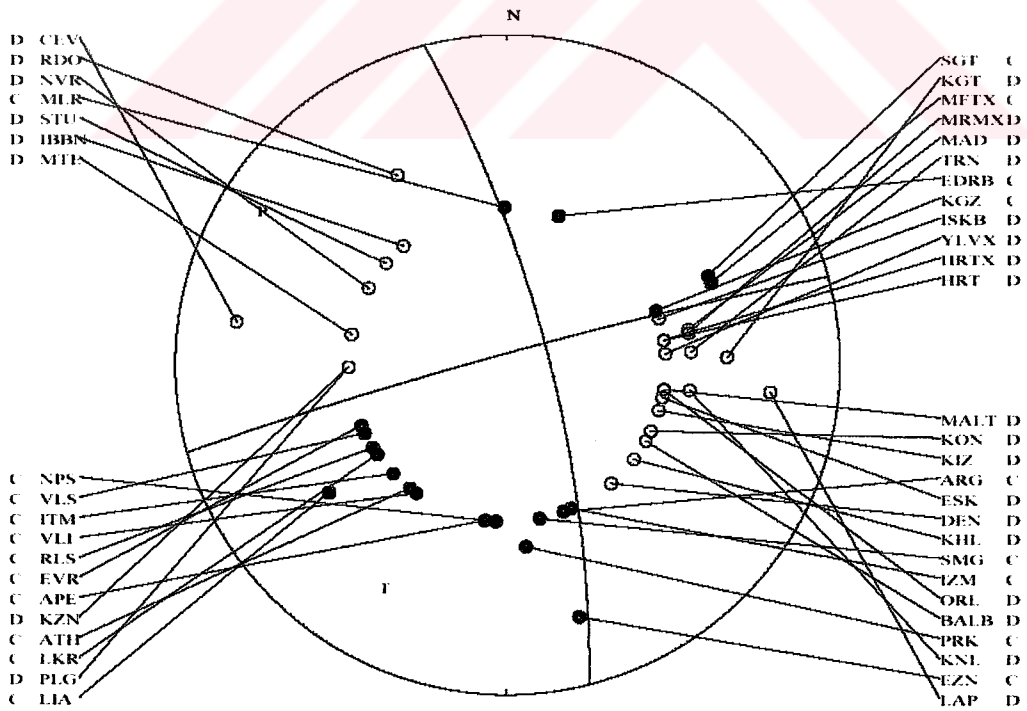
Focal mechanism solutions of fifteen selected earthquakes ($M_L > 3.8$) from the Saros earthquake sequence.



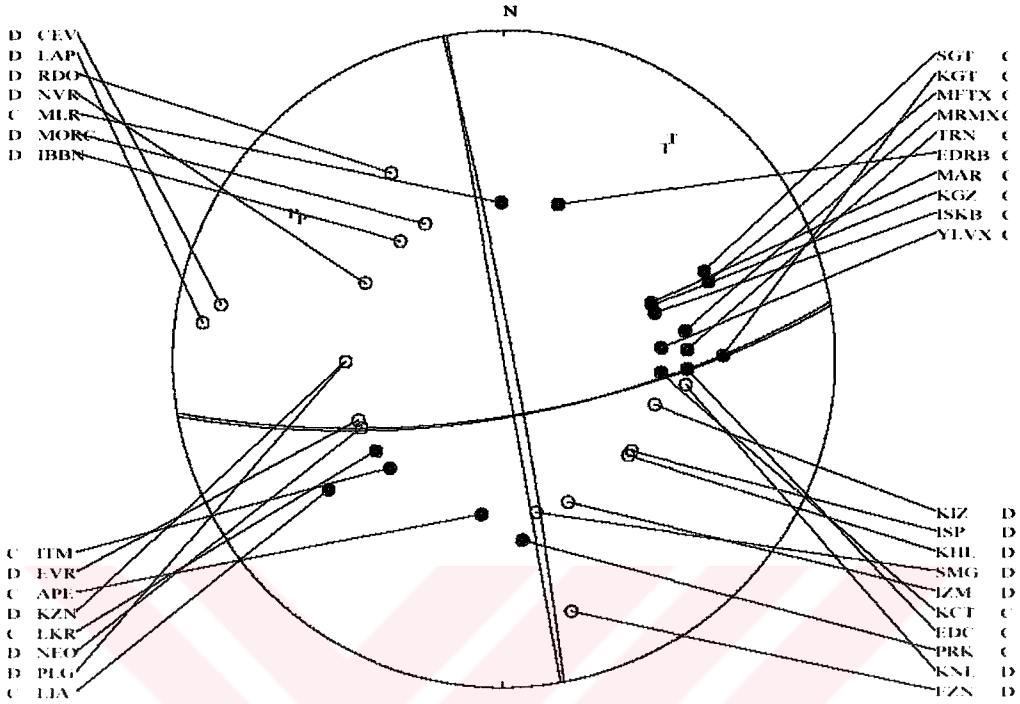
2003 7 5 2158 29.60L 40.441 26.063 11.7 SAR 12 0.1 4.3CSAR
 350.0 60.0 0.0 1



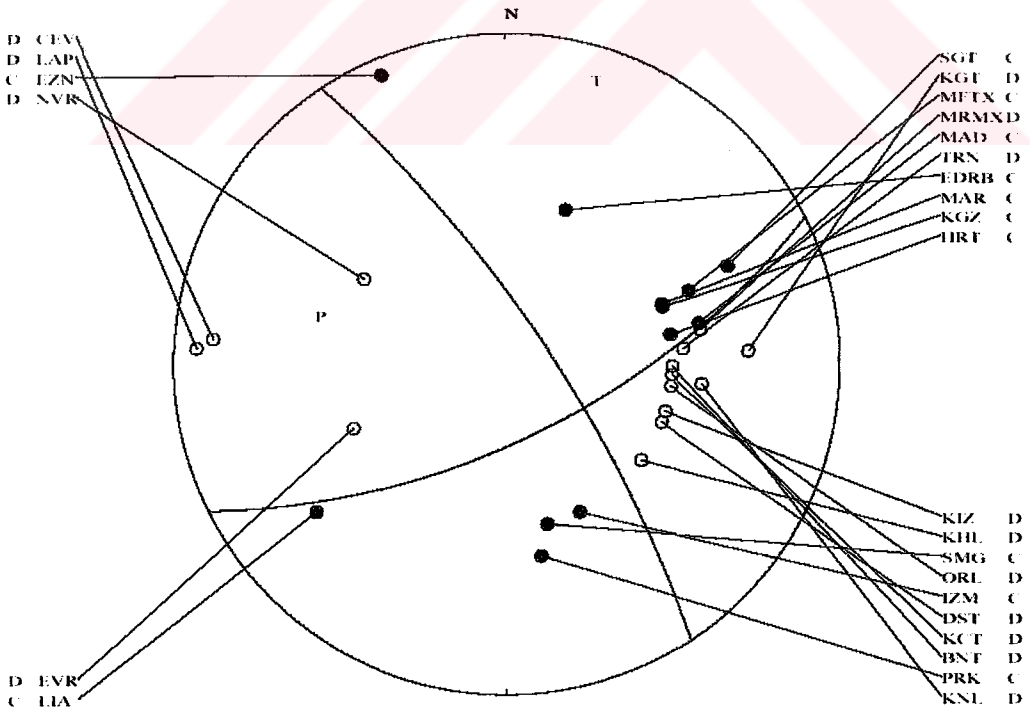
2003 7 6 1910 28.00L 40.427 26.103 17.5 SAR 20 0.1 5.8CSAR
 345.5 75.5 4.0 0



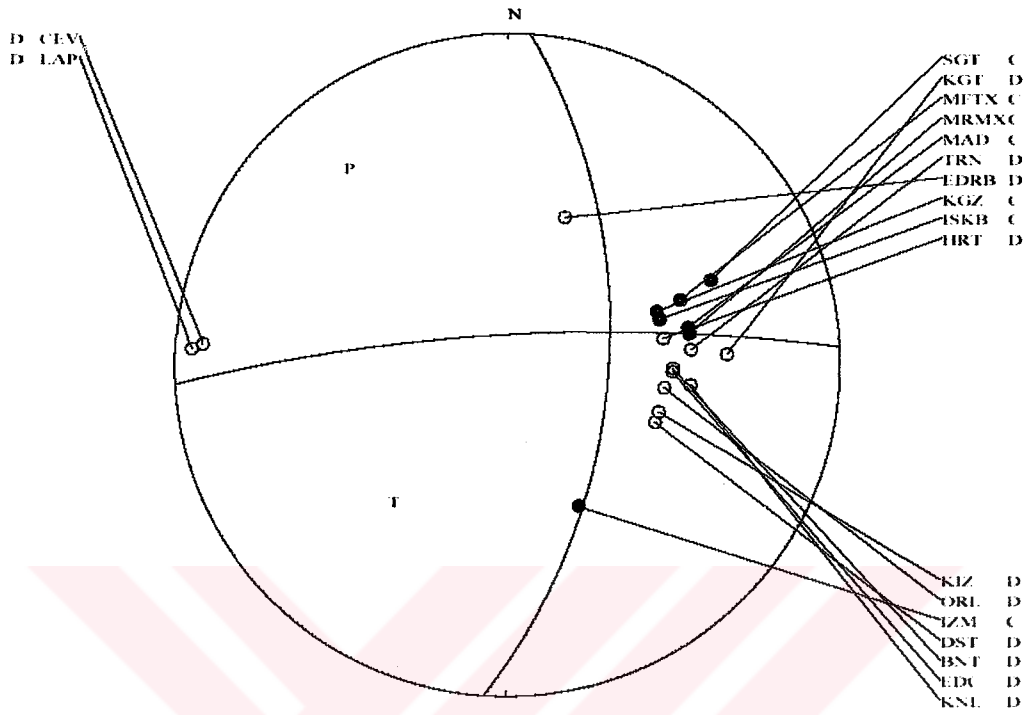
2003 7 6 2010 15,601. 40,439 26,108 16.4 SAR 14 0.1 5.3CSAR
 349.4 86.6 -19.7 1
 170.0 90.0 20.0 1



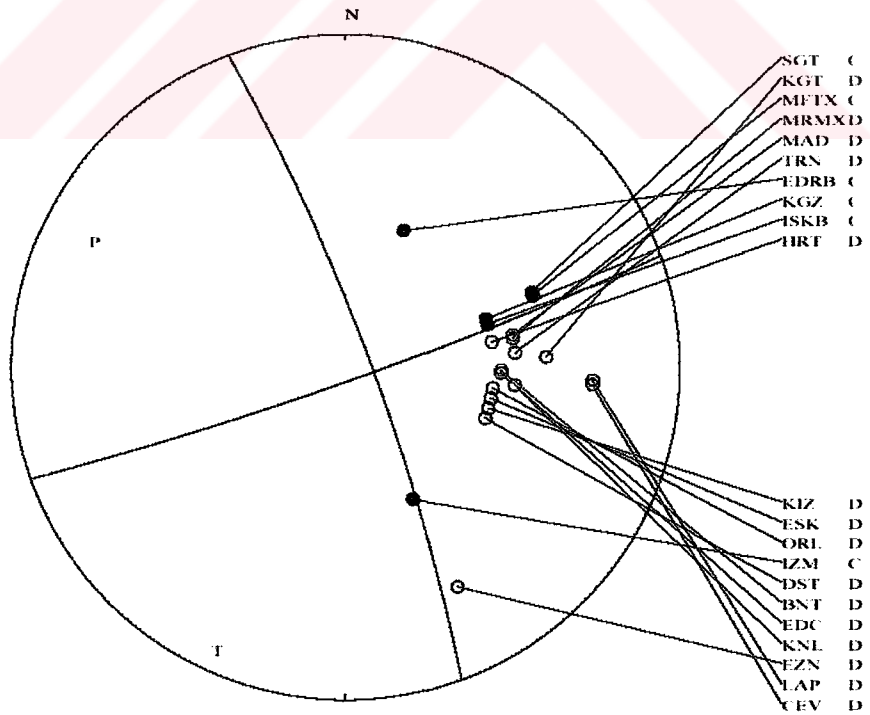
2003 7 6 2048 53,301. 40,406 26,006 19.6 SAR 11 0.1 4.7CSAR
 326.6 75.5 -26.6 0



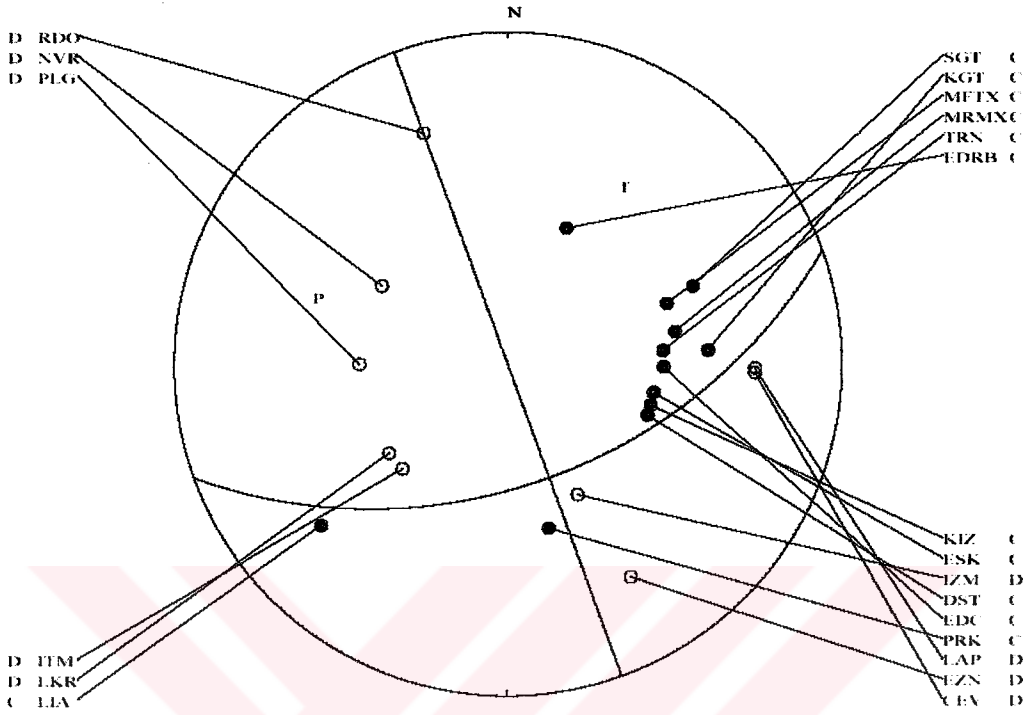
2003 7 6 2205 48,501 40,403 25,989 16.3 SAR 12 0.1 4.2CSAR
 3.9 56.0 12.7 0



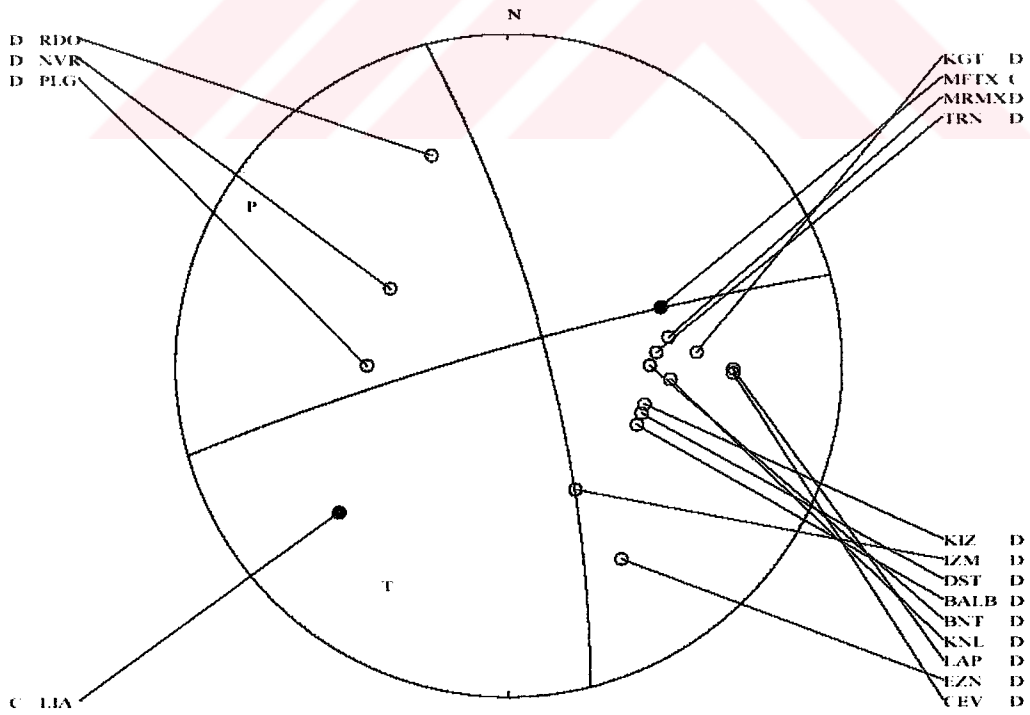
2003 7 6 2242 8,701 40,405 25,940 13.3 SAR 11 0.2 4.4CSAR
 339.6 81.4 5.0 0



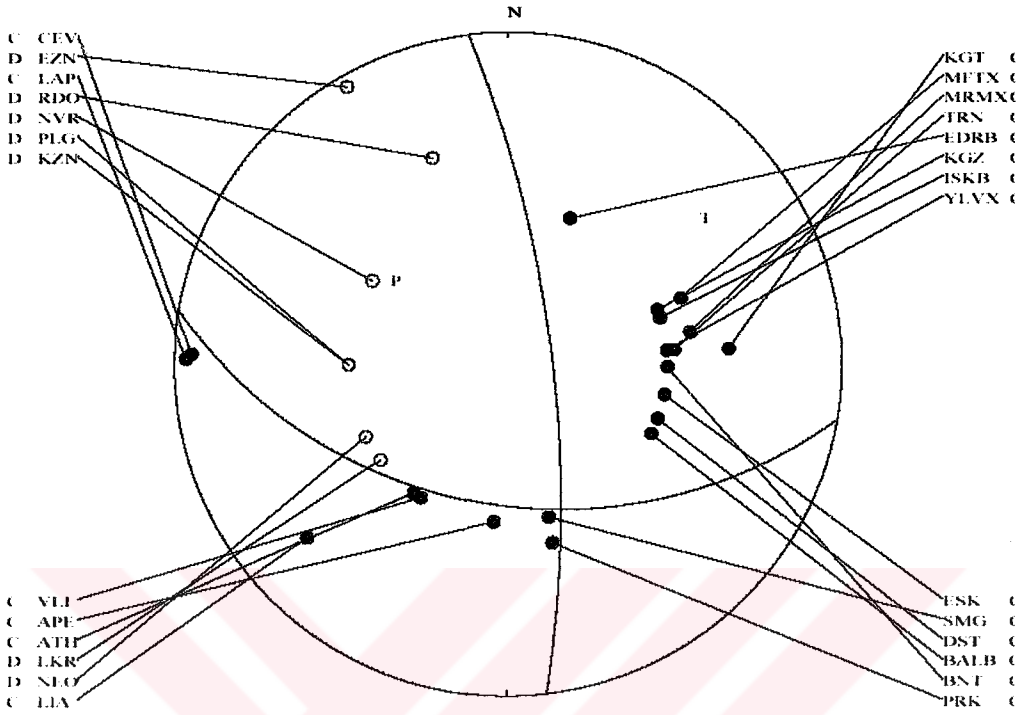
2003 7 9 2201 57.501 40.385 25.913 12.6 SAR 15 0.1 3.8CSAR
 160.0 90.0 40.0 0



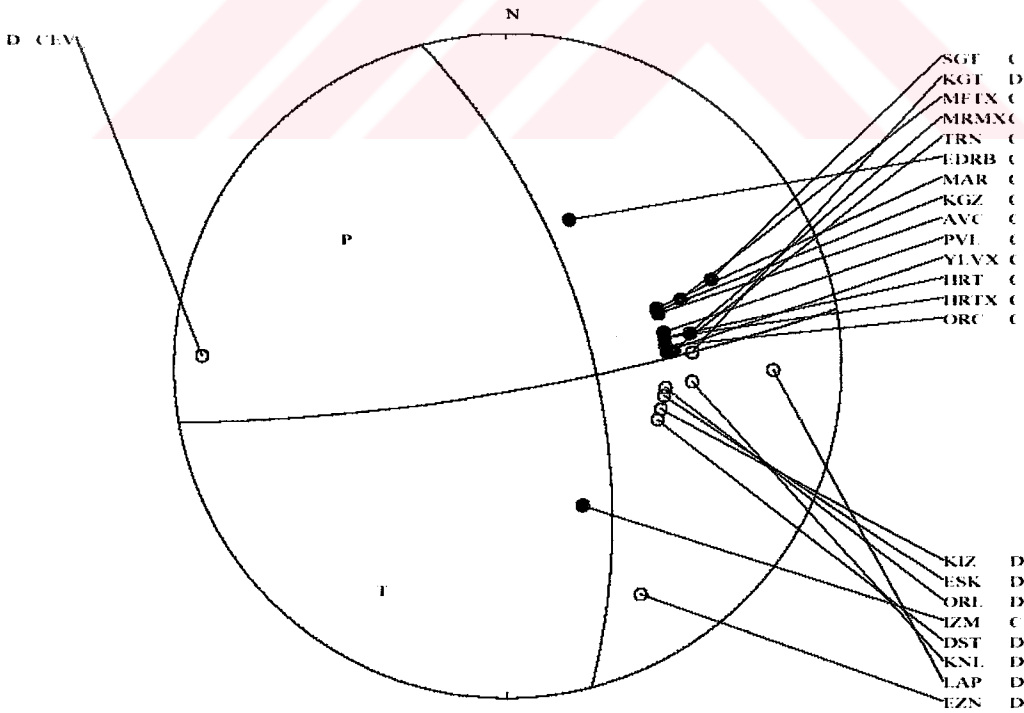
2003 7 9 2208 49.501 40.386 25.902 11.9 SAR 15 0.1 4.1CSAR
 315.8 76.4 6.5 0



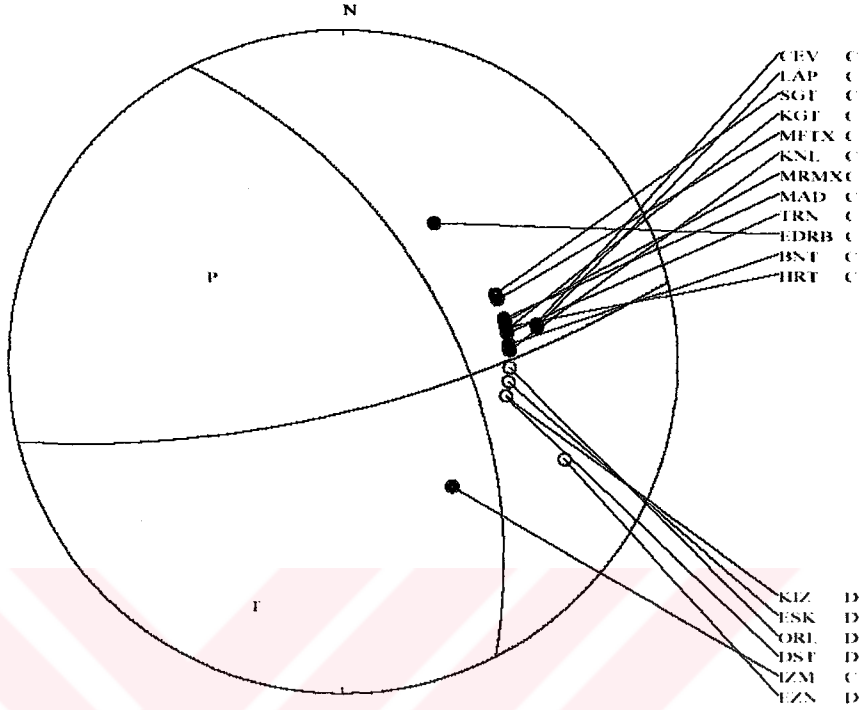
2003 7 9 2231 40.70L 40.388 25.912 15.8 SAR 10 0.1 4.7C SAR
 353.2 74.8 -48.2 0



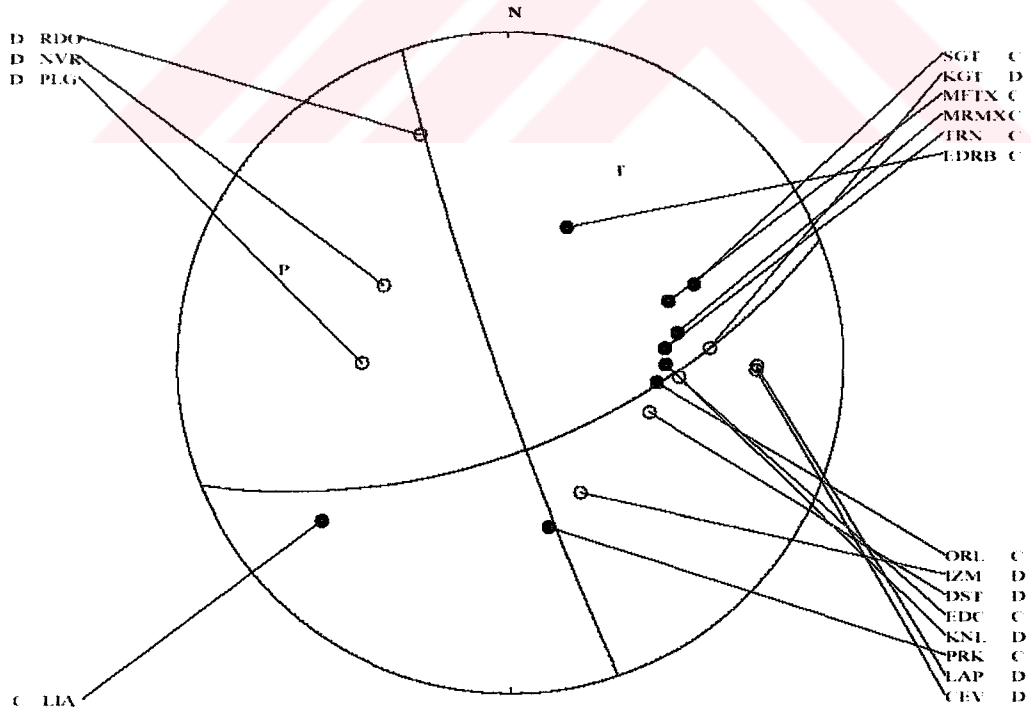
2003 7 10 0126 17.70L 40.387 25.912 16.5 SAR 9 0.2 4.4C SAR
 345.4 61.6 -10.1 0



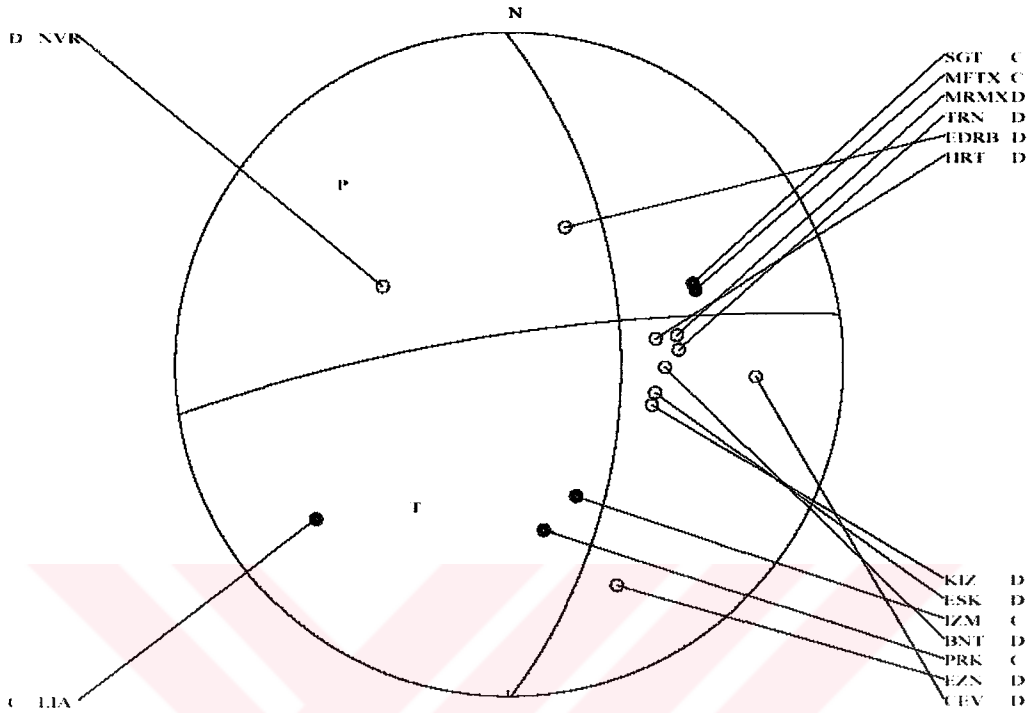
2003 710 0901 17.80L 40.183 25.305 20.7 SAR 9 0.1 4.0C SAR
 332.7 53.0 -21.5 0



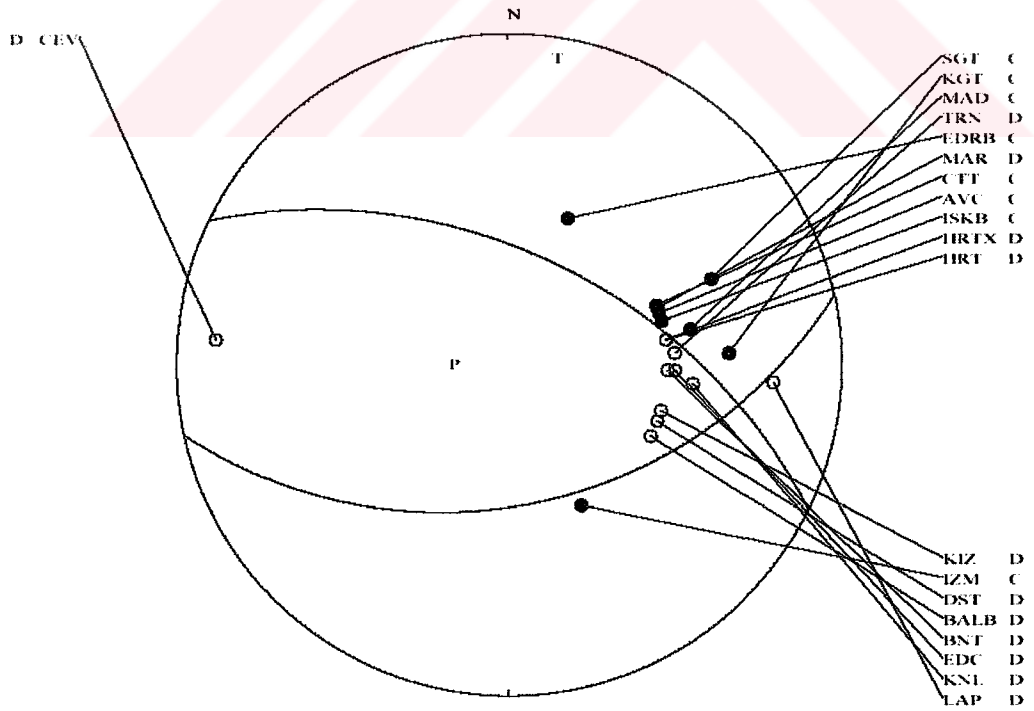
2003 713 0632 8.10L 40.389 25.923 13.9 SAR 15 0.1 4.0C SAR
 161.3 85.0 29.6 0



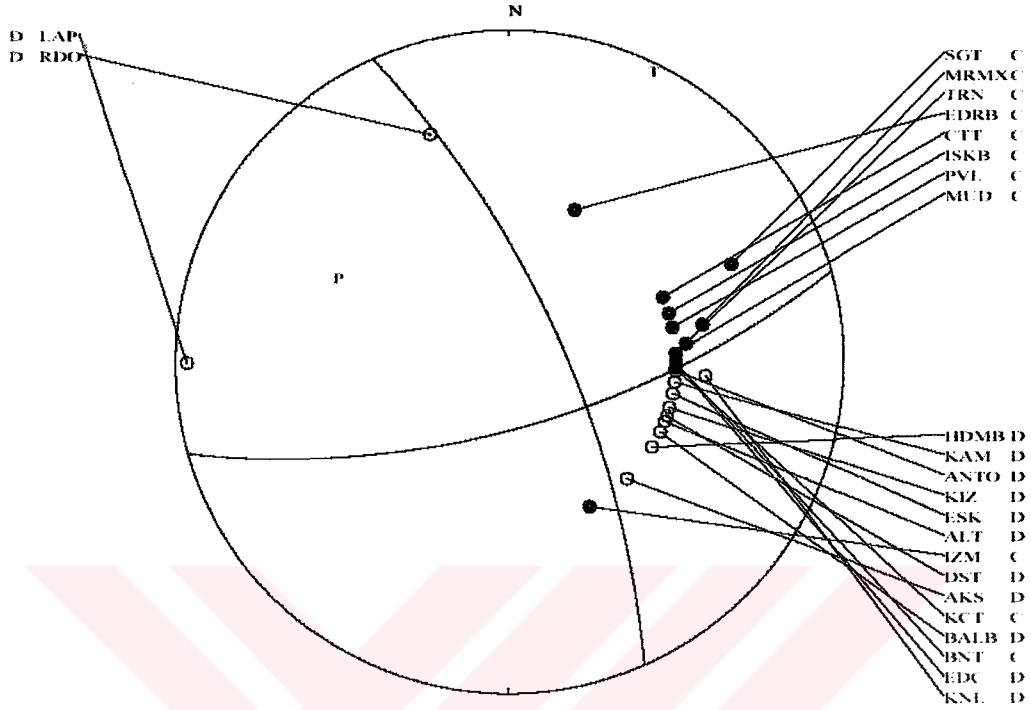
2003 718 0544 7.20L 40.394 25.962 14.0 SAR 12 0.1 3.8CSAR
 359.5 53.0 13.3 0



2003 831 0750 86.70L 40.415 25.972 17.0 SAR 11 0.1 4.0CSAR
 296.0 52.8 -64.6 1



2004 615 1202 38.60L 40.373 25.903 19.1fSAR 12 0.1 5.1fSAR
336.0 71.3 -23.9 1



APPENDIX C

Table C-1: List of stations used in M_S calculations. IU: IRIS/USGS Network, HL: National Observatory of Athens Digital Broadband Network, GE: GEOFON Network: GR: German Network, MN: Mediterranean Very Broadband Seismographic Network, KO: Kandilli Observatory and Earthquake Research Institute Network, IS: Israel Network, NL: Netherlands Seismic Network, PL: Poland Network.

Station Name	Network Code	Latitude (N°)	Longitude (E°)	Elevation (m)	Location	Sensor Type	Digitizer Type
ANTO	IU	39,87	32,79	883	Turkey	VBB	24bit
APE	HL	37,069	25,531	620	Greece	Le3D/20sec	DR-24
APEZ	GE	34,98	24,89	400	Greece	STS-2	Quanterra
AQU	MN	42,354	13,405	710	Italy	STS-2	Q4120
ARG	HL	36,216	28,126	170	Greece	Le3D/20sec	DR-24
BALB	KO	39,6506	27,8642	333	Turkey	CMG-40T	DM24
BNI	MN	45,052	6,678	1395	Italy	STS-2	Q4120
CART	GE	37,5868	-1,0012	65	Spain	STS-2	Q4120
CII	MN	41,723	14,305	910	Italy	STS-2	Q680
CSS	GE	34,962	33,331		Cyprus	STS-2	Quanterra
CUC	MN	39,993	15,815	665	Italy	STS-2	Q4120
DAG	GE	76,771	-18,655		Greenland	STS-2	24bit
DSB	GE	53,245	-6,375	236	Ireland	VBB	24bit
EDRB	KO	41,847	26,7437	209	Turkey	CMG-40T	DM24
EIL	IS	29,6699	34,9512	210	Israel	STS-2	Quanterra
FODE	GE	35,38	24,96	60	Greece	STS-2	Quanterra
FURI	IU	8,9	38,68		Ethiopia	VBB	24bit,HF,LG
GNI	IU	40,05	44,72	1460	Armenia	VBB	24bit,HF
GRFO	GR	49,6909	11,2203	384	Germany	KS-36000	Q380
GVD	GE	34,839	24,09	200	Greece	STS-2	Quanterra
HGN	NL	50,764	5,9317	135	Netherlands	STS-1	16bit
HLG	GR	54,1847	7,8839	41	Germany	STS-2	PS2400
HRTX	KO	40,8009	29,673	614	Turkey	L4-3D	HRD24
IBBN	GE	52,3072	7,7516	140	Germany	STS-2	Q380
IDI	MN	35,288	24,89	750	Greece	STS-1	Q380
ISKB	KO	41,0639	29,06	132	Turkey	CMG-3T	DM24
ISP	GE	37,8433	30,5093	1100	Turkey	STS-1	Q380
ITM	HL	37,1786	21,9252	400	Greece	Le3D/20sec	DR-24
JER	IS	31,7719	35,1972	770	Israel	STS-2	Quanterra
KBS	IU	78,9256	11,9417	77	Norway	VBB	24bit,HF
KEK	HL	39,71	19,8	280	Greece	Le3D/20sec	DR-24
KIEV	IU	50,69	29,21	163	Ukraine	VBB	24bit,HF,LG

KMBO	IU	-1,1268	37,2523	1960	Kenya	STS-2	Unknown
KONO	IU	59,6491	9,5982	216	Norway	STS-1	24bit
KRIS	GE	35,178	25,503		Greece	STS-2	Quanterra
KSDI	IS	33,192	35,6576	123	Israel	STS-2	Quanterra
KWP	PL	49,6314	22,7075	448	Poland	STS-2	Q680
MAHO	GE	39,8959	4,2665	25	Spain	STS-2	Q4120
MALT	GE	38,3134	38,4273	1120	Turkey	STS-2	Quanterra
MELI	GE	35,2899	-2,9392	40	Spain	STS-2	Q380
MHV	GE	54,96	37,77	150	Russia	VBB	24bit
MLSB	KO	37,31	27,79	NA	Turkey	CMG-40T	DM24
MORC	GE	49,7766	17,5428	740	Czech Rep.	STS-2	Quanterra
MRMX	KO	40,6089	27,5831	741	Turkey	CMG-40T	HRD24
MRNI	IS	33,1178	35,392	918	Israel	STS-2	Quanterra
MTE	GE	40,4	-7,54		Portugal	VBB	24bit
PSZ	GE	47,9184	19,8944	940	Hungary	STS-2	Quanterra
RDO	HL	41,146	25,538	100	Greece	Le3D/20sec	DR-24
RGN	GE	54,5477	13,3214	15	Germany	STS-2	Q380
RUE	GE	52,4759	13,78	40	Germany	STS-2	Q380
SANT	GE	36,371	25,459		Greece	STS-2	Quanterra
SFS	GE	36,4656	-6,2055	21	Spain	STS-2	Unknown
SFUC	GE	36,637	-6,175	88	Spain	STS-2	Q380
SKD	GE	35,412	23,928	306	Greece	STS-2	Unknown
STU	GR	48,7705	9,1933	360	Germany	STS-2	Q4120
SUMG	GE	72,5763	-38,4538	3275	Greenland	BB	Unknown
SUW	PL	54,0125	23,1808	152	Poland	STS-2	Quanterra
SVSK	KO	39,9157	36,992	1400	Turkey	CMG-40T	DM24
TIP	MN	39,179	16,758	815	Italy	STS-2	Q4120
TIRR	GE	44,4581	28,4128	77	Romania	STS-2	PS6-24
TRI	MN	45,709	13,764	161	Italy	STS-1	Q4120
TRTE	GE	58,3786	26,7205	100	Estonia	STS-2	Q380
VANB	KO	38,595	43,3888	1750	Turkey	CMG-3T	DM24
VLC	MN	44,159	10,386	555	Italy	STS-2	Q4120
VSL	MN	39,496	9,378	370	Italy	STS-1	Q4120
VSU	GE	58,462	26,7347	63	Estonia	STS-2	Quanterra
VTS	MN	42,618	23,235	1490	Bulgaria	STS-1	Q380
WDD	MN	35,867	14,523	41	Malta	STS-2	Q680
WLF	GE	49,6646	6,1526	295	Luxemburg	VBB	Quanterra
WTSB	NL	51,9663	6,7989	43	Netherlands	STS-2	16bit
YLVX	KO	40,5667	29,3728	860	Turkey	CMG-40T	HRD24
ZKR	GE	35,1147	26,217	270	Greece	STS-2	Unknown



The Analysis of 2003 Saros Earthquake Sequence, North Eastern Aegean Region

A.Kamec Mutlu¹, H. Karabulut¹, S. Ozalaybey², A. Kratzl³, M. Aktar¹, R. Roumeliate³, C. Benetatos³, C. Tapirdamaz²

¹ Bogaziçi University, Kandilli Observatory and Earthquake Research Institute, TR- Istanbul, Turkey

² TUBITAK-MAM, Marmara Research Center, Earth and Marine Sciences Institute, TR- Gebze, Turkey

³ Aristotle University of Thessaloniki, Thessaloniki, Greece



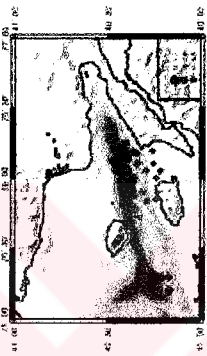
We study the seismotectonics of the Gulf of Saros by studying the aftershock activity following Mw=5.8, 6 July, 2003 earthquake. The earthquake took place at a depth of 18 km on the continuation of the North-Anatolian Fault Zone (NAFZ) from the western Marmara Sea into the Gulf of Saros. The mechanism was almost pure right lateral strike slip with a strike direction of N17E. The activity occurred along the axis of the gulf between the depths of 7 km and 20 km. Focal mechanism of main shock and largest aftershock are almost pure right lateral strike slip aligned with the axis of Saros depression. Eastern extent of the activity marks a long term seismic quiescence observed as a result of 1912 Ganos Earthquake Mw=7.4. We present results from these analysis and discuss the seismotectonic implications on the continuation of the North-Anatolian Fault System and the North Eastern Aegean Trough.



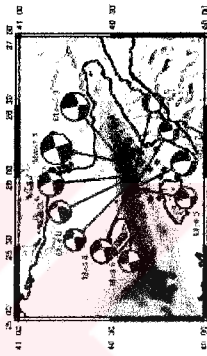
Regional map showing the location of the permanent stations operated by the National Observatory of Athens (♦) TUBITAK, Marmara Research Center (▲) and Bogaziçi University Kandilli Observatory and Earthquake Research Institute (▲).



The seismic activity along the North Anatolian Fault Zone indicates continuous deformation (NEIC Catalog). The segment at which 1912 Tokat-Sakarya earthquake (Mw=7.4) took place (July 06, 2003 (Mw=5.8), Saros earthquakes occurred on the westernmost end of this segment.



Map view and depth view of the located events following the Saros earthquake between the dates 6 July, 2003 and 9 September, 2003. Local magnitudes were computed by using broadband recordings.



Lower hemisphere projection of focal mechanisms of the main shock and large aftershocks ($M_w > 3.0$).

DISCUSSION

A close look at the distribution of epicenters clearly shows that both the main shock and aftershocks are located along the deep trough that forms the axis of the Saros Bay depression. No seismic activity is detected on the northern strand which may be the evidence for a stable non-slipping zone on the north of the Saros Bay extending with the 20 km strike-slip zone on the southern part of the depression. In fault plane solutions, the dominant right lateral strike-slip with minor normal components are aligned with the axis of the Saros depression. There are also the east-trending Anatolian Fault. A relatively deep aseismic zone which reaches 20 km clearly indicates that the activity is occurring well below the branching point of the lower structure (Kurt et al., 2000). This observation is not totally unexpected since a similar characteristic was also observed at the western end of the Marmara Sea (Çampanyı et al., 2003). Another consideration is related to the argument of whether the well located swarm activity may represent the western limit of the 1912 rupture, which is recognized that a consistent seismic quiescence line has established along the rupture length of the 1912 Ganos Earthquake (M=7). Although the full length of the seismic line across the Ganos Fault agrees well with the axis of the basin, the exact location of the rupture ends will always be debatable. The swarm data presented in this paper, unlike the earlier data, have the locations accuracies of the order of 1-2 km. In horizontally, therefore, indicate a well defined western limit to the quiescence line. The data presented in this study, which is constrained to the analysis of a temporary swarm activity, is far from providing a decisive evidence for the above conjecture and more observations and discussions are needed in order test its validity.

Mert K. Demirel, B. Mustafa I. Akinci, Erdemir, Kocabaş and Demirel of the Dept. of Earth and Space Sciences, Bogaziçi University, Kandilli Observatory and Earthquake Research Institute, 192 00011, Istanbul, Turkey. E-mail: murtk@boga.istanbul.bogaziciuni.edu.tr, erdemir@boga.istanbul.bogaziciuni.edu.tr, kocubas@boga.istanbul.bogaziciuni.edu.tr, demirel@boga.istanbul.bogaziciuni.edu.tr

ACKNOWLEDGMENTS

We thank National Observatory of Athens, TUBITAK Marmara Research Center and Bogaziçi University Kandilli Observatory and Earthquake Research Institute for providing data. Thank Eren Apat for his suggestions. Maps in this study were plotted by GMT software of Wessel and Smith (1995). This project was supported by TUBITAK Y0BAG-1027013